November 7, 1974

To the Graduate Council:

I am submitting herewith a thesis written by Lynn Hugh Malone entitled "Comparison of the Electron-Ion Recombination Rate to the Gas Dynamics Expansion Rate in an Expanding Argon Plasma." I recommend that it be accepted in partial fulfillment of the requirements for the degree of Master of Science, with a major in Physics.

Arthur A. Mason

Arthur A. Mason, Major Professor

We have read this thesis
and recommend its acceptance:

Roy D Joseph

W A Dunnill

Accepted for the Council:

Hilton A. Smith

Vice Chancellor
Graduate Studies and Research

COMPARISON OF THE ELECTRON-ION RECOMBINATION RATE TO THE GAS DYNAMICS EXPANSION RATE IN AN EXPANDING ARGON PLASMA

A Thesis

Presented for the

Master of Science

Degree

The University of Tennessee

Lynn Hugh Malone

March 1975

ACKNOWLEDGMENTS

The author wishes to express his appreciation to Dr. W. K. McGregor, Engine Test Facility, ARO, Inc., discussions with whom provided the basis for this study, and to Dr. C. C. Limbaugh, Engine Test Facility, ARO, Inc., for his many suggestions and recommendations.

Special thanks also are due to Messrs. R. J. Bryson and J. D. Few, Engine Test Facility, ARO, Inc., for their technical advice and information.

Also, the author is indebted to Dr. A. A. Mason, Professor of Physics, The University of Tennessee Space Institute, for his general support of this study.

The research reported herein was sponsored by Headquarters, Air Force Systems Command, Arnold Engineering Development Center, Arnold Air Force Station, Tennessee, within the terms of Contract F40600-75-C-0001 with ARO, Inc. Further reproduction is authorized to satisfy the needs of the United States Government.

1207212

ABSTRACT

Many investigators have determined the collisional-radiative recombination (CRR) coefficient of argon both experimentally and theoretically. However, the present methods employed to determine the CRR coefficient are quite involved. A more direct method for determining the CRR coefficient by measurements of electron density in an expanding plasma flow has been proposed. The purpose of this study was to examine the feasibility of using this method in determining the CRR coefficient for argon in the partially ionized plume from an arcjet.

In order for experimental measurements to produce meaningful data for direct determination of the CRR coefficient, the CRR mechanism must dominate the gas dynamic (GD) mechanism. Computer calculations coupling the two rate mechanisms were made and were compared with experimental data which were available. In the range of stagnation conditions studied theoretically (1300°K $\leq$ gas temperature $\leq$ 2800°K; 8.27×10^{13} 1/cm^3 $\leq$ electron number density $\leq$ 5.00×10^{18} 1/cm^3; and 8000°K $\leq$ electron temperature $\leq$ 20,000°K) the GD rate dominated over the CRR rate. It was determined that it would require approximately complete ionization for the CRR rate to dominate the GD rate.

Analysis of available experimental data confirmed the theoretical results, showing that the physical conditions existing in the arcjet plume required more detailed methods for complete description.

TABLE OF CONTENTS

CHAPTER		PAGE
I.	INTRODUCTION	1
	Background	2
	Experimental Determination of Recombination Rates	5
	Microwaves	6
	Laser interferometric method	7
	Spectroscopy	10
	Theoretical Calculations	11
II.	THE RECOMBINATION COEFFICIENT	13
	Introduction	13
	Collisional-Radiative Recombination	13
III.	COLLISIONAL-RADIATIVE RECOMBINATION VERSUS GAS DYNAMICS	21
	Introduction	21
	Coupled Collisional-Radiative Recombination with Gas Dynamics	21
	Initial Conditions	30
	Results	32
	Electron Number Density	42
IV.	EXPERIMENTAL DATA	46
	Introduction	46
	Apparatus and Procedure	46
	Analysis	52

CHAPTER PAGE

Theoretical Comparisons. 64

V. SUMMARY AND CONCLUSIONS. 69

BIBLIOGRAPHY 71

VITA 75

LIST OF FIGURES

FIGURE PAGE

1. Electron Temperature Variation on the Axis of an Expanding Argon Plasma Jet; Initial Electron Temperature of 17,000°K [23]. 31

2. Collisional-Radiative Recombination Rate and Gas Dynamic Rate versus Time; Initial Gas Temperature of 1365°K, Initial Electron Number Density of 3.31×10^{14} $1/cm^3$, and Electron Temperature (at x/D = 1.001) of 15,700°K. . . . 34

3. Collisional-Radiative Recombination Rate and Gas Dynamic Rate versus Time; Initial Gas Temperature of 2222°K, Initial Electron Number Density of 4.52×10^{14} $1/cm^3$, and Electron Temperature (at x/D = 1.001) of 15,900°K. . . . 35

4. Collisional-Radiative Recombination Rate and Gas Dynamic Rate versus Time; Initial Gas Temperature of 2715°K, Initial Electron Number Density of 8.27×10^{13} $1/cm^3$, and Electron Temperature (at x/D = 1.001) of 16,000°K. . . . 36

5. Collisional-Radiative Recombination Rate and Gas Dynamic Rate versus Time; Initial Gas Temperature of 1365°K, Initial Electron Number Density of 3.31×10^{16} $1/cm^3$, and Electron Temperature (at x/D = 1.001) of 16,000°K. . . . 38

FIGURE PAGE

6. Collisional-Radiative Recombination Rate and Gas Dynamic Rate versus Time; Initial Gas Temperature of 2715°K, Initial Electron Number Density of 3.45×10^{17} $1/cm^3$, and Electron Temperature (at x/D = 1.001) of 15,700°K. . . . 40

7. Ratio of Collisional-Radiative Recombination Rate to Gas Dynamic Rate; Initial Gas Temperature of 2715°K and Electron Temperature (at x/D = 1.001) of 16,000°K (Using Equation (45) for Determining T_e). . . . 41

8. Ratio of Collisional-Radiative Recombination Rate to Gas Dynamic Rate; Initial Gas Temperature of 2715°K and Electron Temperature (at x/D = 1.001) of 16,000°K (Using Reference [23] for Determining T_e) . . . 43

9. Electron Number Density and Electron Number Density when Collisional-Radiative Recombination Rate Equals the Gas Dynamic Rate versus x/D. 45

10. Plasma Jet and Test Cell Schematic [27] 48

11. Electronic Sketch 50

12. Raw Data (Intensity) Scans for a Wavelength of 4158 Å at a Position (x/D) of 3.0 53

13. Raw Data (Intensity) Scans for a Wavelength of 4158 Å at a Position (x/D) of 4.0 54

FIGURE PAGE

14. Raw Data (Intensity) Scans for a Wavelength of 4158 Å at a Position (x/D) of 5.0 55

15. Raw Data (Intensity) Scans for a Wavelength of 6032 Å at a Position (x/D) of 3.0 56

16. Raw Data (Intensity) Scans for a Wavelength of 6032 Å at a Position (x/D) of 4.0 57

17. Raw Data (Intensity) Scans for a Wavelength of 6032 Å at a Position (x/D) of 5.0 58

18. Normalized Emission Coefficient at a Position (x/D) of 3.0 59

19. Electron Temperature along the Centerline as Calculated from Intensity Measurement 61

20. Electron Number Density along the Centerline as Calculated from Intensity Measurement 63

21. Collisional-Radiative Recombination Rate and Gas Dynamic Rate versus Time; Initial Gas Temperature of 4890°K, Initial Electron Number Density of 3.45×10^{17} $1/cm^3$, and Electron Temperature (at x/D = 1.001) of 17,300°K. . . . 67

NOMENCLATURE

A	Transition probability from q to p ($q > p$), 1/sec
$\bar{A}$	Transition probability from p to q ($p > q$), 1/sec
A'	Empirical constant
B	Geometric constant
C	Empirical constant
c'	Calibration factor, $\frac{\text{watts}}{\text{ster. cm}^2}$ div.
c	Continuum
c_s	Speed of sound, cm/sec
D	Diameter of nozzle, cm
D_a	Ambipolar diffusion coefficient, cm^2/sec
E	Excitation energy, eV
e	Charge of electron, 4.80286×10^{-10} statcoulomb
e^-	Electron
g	Statistical weight
$H(p)$	Total rate of atoms leaving state p by three body recombination or de-excitation, cm^3/sec
h	Planck's constant, 6.62517×10^{-27} ergs/sec
I_p	Ionization potential of level p, eV
$K(c,P)$	Rate coefficient for three body recombination into level p, cm^3/sec

$K(p,c)$	Rate coefficient for the reverse of the three body recombination, cm^3/sec
$K(p,q)$	Rate coefficient for excitation or de-excitation from level p to level q, cm^3/sec
$K(q,p)$	Rate coefficient for excitation or de-excitation from level q to level p, cm^3/sec
k	Boltzmann constant, 8.6164×10^{-5} eV/°K
L	Ratio of electron number density to atom number density
M	Mach number
m_e	Mass of electron, 9.1083×10^{-28} g
m_A	Mass of argon atom, 6.630×10^{-23} g
N	Atom
N^+	Ion
$n(c)$	Electron number density, $1/cm^3$
$\overline{n(c)}$	Average electron number density, $1/cm^3$
$n(N)$	Atom number density, $1/cm^3$
$n(N)'$	Total heavy particle number density, $1/cm^3$
$n(N^+)$	Ion number density, $1/cm^3$
P	Pressure, torr
p	Quantum number
Q	Cross section, cm^2
q	Quantum number
R	Gas constant, 8.31662×10^7 erg/(g mole)/°K

S	Collisional-radiative ionization coefficient, cm^3/sec
S'	Difference in the distance along the centerline divided by the diameter of the nozzle
T_e	Electron temperature, °K
T_g	Gas temperature, °K
T_0	Stagnation temperature, °K
t	Time, sec
u	Nondimensional excitation energy
V	Volume, cm^3
v	Velocity of flow, cm/sec
X	Ratio of electron number density to ion number density
x	Distance from nozzle along centerline, cm
Y	Represents some third body in three body recombination
Z	Refers to the level of ionization
$\alpha_{CRR}(n(c),T_e)$	Collisional-radiative recombination coefficient, cm^3/sec
$\beta(p)$	Rate coefficient for radiative recombination, cm^3/sec
Γ	Collisional-radiative decay coefficient, cm^3/sec
γ	Ratio of specific heats, 1.67 for argon
ϵ_f	Permittivity of free space, 8.85×10^{-4} farad/cm

θ	Term denoting gas dynamic effects on ratio of electron density at two points along the centerline
λ	Resonant wavelength, Å
μ_p	Index of refraction of the plasma
ν	Frequency, 1/sec
ρ	Total mass density, g/cm^3
σ	Ratio of atom number density to equilibrium atom number density
τ	Mean time due to diffusion, sec
ϕ	Term denoting part of the gas dynamic rate of change on the electron number density
ω	Angular frequency, 1/sec

Subscripts

1,2	Refers to two points in the flow along the centerline
i,j	Refers to energy levels
0	Refers to initial values

CHAPTER I

INTRODUCTION

There is a continuing need for a more complete description of various nonequilibrium phenomena in high speed gas flows. Many of these nonequilibrium phenomena can be observed in the freely expanding, partially ionized plasma from an arcjet. Since the plume of an arcjet contains ionized specie, studies which use the plume must include considerations of the effects due to the recombination processes. These effects are generally described by the use of a recombination rate coefficient, for which there are several methods of determination. These methods, described in more detail below, are quite involved and are subject to interpretation.

Knowledge of the recombination process at the conditions in the plume at the points of observation is required for studying nonequilibrium processes in the arcjet plume. Further, a simple means of determining the recombination rate coefficient would enhance such studies. Therefore, it was decided to conduct a study of the expected effects due to the purely recombination process coupled to the purely gas dynamic process for an argon arcjet. The coupling is accomplished in an elementary manner, but such an analysis does give order of magnitude comparison of the

coupled processes. It also provides a feasibility study into one method of use of the arcjet plume for determining the recombination rate coefficient in a nonequilibrium environment.

I. BACKGROUND

A free electron and a positive atomic ion are said to recombine if they interact to form a neutral atom, either in the ground state or in an excited state. This event is called electron-ion recombination. A more general description of recombination is that of a charge-neutralizing encounter between charge carriers of opposite sign, but the name is misleading because the two particles were generally never previously together. This true recombination in which the electrons and ions were originally together may be important only at short times after ionization and before the electrons and positive ions can escape their mutual attractive field [1].[1]

Since the particles can be considered free before recombining, the recombination process has an excess of energy which must be disposed of in order to satisfy the conservation laws. If no third body is present, the energy liberated may be carried off as radiation. This loss mechanism of free electrons from the plasma is commonly

---

[1]Numbers in brackets refer to similarly numbered references in the bibliography.

called radiative recombination, and can be described with the chemical equation

$$N^+ + e^- \rightarrow N^* + h\nu \ , \qquad (1)$$

where the superscript + indicates the ion and the superscript * indicates the recombined atom in some excited state (which can undergo further transitions due to collisional de-excitation or even ionization), e^- represents the electron, and $h\nu$ is the energy carried off by radiation. In general, this loss mechanism only describes the actual recombination if the plasma is sufficiently tenuous such that binary collisions dominate [1]. When dealing with dense plasmas, where three body collisions are important, the role of the third body in carrying off the excess energy of recombination must be taken into account [1]. This process is called collisional recombination and can be written as

$$N^+ + e^- + Y \rightarrow N^* + Y \ , \qquad (2)$$

where Y represents the third body that carries off the excess energy.

A third possible process involved in electron-ion recombination is called dielectronic recombination. The electron is captured by the ion (N^+) into some excited state of the recombined atom (N^*), and the excess energy is taken up by a second electron (of the recombined atom) which then

moves into an excited state. The doubly excited state N_d^* thus formed is unstable and may revert to the N^+ state by autoionization (autoionization is where one of the electrons drops to a lower energy level and the resulting de-excitation energy is used to eject the other excited electron from the atom without releasing any radiation). If, however, the N_d^* state undergoes a radiative transition and drops down to some state N_b then dielectronic recombination is said to have occurred [1]. This reaction is written as

$$N^+ + e^- \rightarrow N_d^* \rightarrow N_b + h\nu \ . \qquad (3)$$

The rate of dielectronic recombination will usually be small because of the relative inefficiency of the second step of the reaction in Equation (3) as compared with the inverse of the first step [1]. Therefore, this reaction can be ignored.

Pure collisional and pure radiative recombination are the extreme cases of a more general loss mechanism which has been termed by Bates, Kingston, and McWhirter [2], as collisional-radiative recombination (CRR). This general loss mechanism is not simply the sum of the two processes, but is an interacting of the collisional and radiative processes. This interaction complicates the study of recombination, which Bates, et al. [2], could describe only by a statistical method.

Usually, the recombination process is described mathematically through the equation

$$\frac{dn(c)}{dt} = - \alpha_{CRR}(n(c),T_e)[n(c)n(N^+)] \ , \qquad (4)$$

where $\alpha_{CRR}(n(c),T_e)$ (with units of cm^3/sec) is the collisional-radiative recombination coefficient (which is a function of the electron number density and T_e , the electron temperature), $n(c)$ (with units of $1/cm^3$) is the electron number density, and $n(N^+)$ (with units of $1/cm^3$) is the ion number density [1]. Assuming a balance of charge ($n(c) = n(N^+)$), Equation 4 can be rewritten as

$$\frac{dn(c)}{dt} = - \alpha_{CRR}(n(c),T_e)[n(c)]^2 \ . \qquad (5)$$

II. EXPERIMENTAL DETERMINATION OF RECOMBINATION RATES

Determining the value of $\alpha_{CRR}(n(c),T_e)$ for different gases has been the subject of numerous studies [3-12]. Various techniques have been used to determine $\alpha_{CRR}(n(c),T_e)$. The use of microwaves [3-9] or laser interferometry [10, 11] has improved the accuracy of determining the CRR coefficient. Spectroscopy also is in use for determining $\alpha_{CRR}(n(c),T_e)$ [12].

Microwaves

Since the late 1940's, the use of microwaves for breaking down a gas and probing the resulting plasma has become a useful tool for experimental studies of recombination. The first use of microwaves for determining the recombination coefficient was made by Biondi and Brown [3, 4] on helium. They measured the mean decay time of charge density in a container of known dimensions by observing the change of the resonant wavelength of a microwave cavity enclosing the container.

Biondi and Brown relate the change in resonant wavelength to the electron number density by

$$\Delta\lambda = B\lambda^2 \overline{n(c)} , \tag{6}$$

where B is a geometric term which takes into account the distribution of the electron number density and electric field in the cavity, $\overline{n(c)}$ is the average electron number density in the cavity, and λ is the resonant wavelength.

The electron number density is determined by measuring

$$\frac{\Delta\lambda}{\lambda^2}$$

as a function of time and substituting into Equation (6). The reciprocal density is plotted versus time, and the CRR coefficient can be determined from the slope of this plot. However, under certain conditions where diffusion losses

outweigh the losses due to recombination, the rate of decay of the electron number density is given approximately by

$$\frac{\partial n(c)}{\partial t} = - \frac{n(c)}{\tau} - \alpha_{CRR}(n(c), T_e)[n(c)]^2 , \qquad (7)$$

where τ is the mean time due to diffusion, and the recombination coefficient must be calculated from Equation (7).

Diffusion becomes important at the walls of the cavity and caution must be used in interpretation of the results. Oskam [5] has emphasized the inapplicability of this method at high power levels of the probing signal because of heating effects and the possibility of secondary electron production. Despite these disadvantages the use of microwaves can yield reliable values of the recombination coefficient under certain conditions. Since Biondi and Brown [3, 4] first used this method other investigators have improved on the experimental values of the recombination coefficient for He and expanded the studies to include other rare gases (Ne, Ar, Kr, and Xe). The list of investigators includes Redfield and Holt [6], Oskam and Mittelstadt [7], and Chen [8, 9]. Although the list is not complete, additional references are cited in Reference [1].

Laser Interferometric Method

Gusinow, Gerardo, and Verdeyen [10] have used laser interferometry to measure the recombination coefficient in helium and argon. The plasma is placed in the

laser cavity rather than in the reference cavity. Because of this a change in the plasma refractivity produces a change in the laser frequency. Gerardo and Verdeyen [11] have shown that by using a spherical mirror in the reference cavity, very small frequency changes can be measured.

The free electrons and neutral atoms are the main contributors to the refractivity at optical wavelengths in a partially ionized gas. The time varying plasma refractivity at optical wavelengths for argon is

$$\mu_p - 1 = (1.03\text{x}10^{-23})n(N) - \frac{1}{2}\frac{n(c)e^2}{m\epsilon_f\omega^2}, \qquad (8)$$

where μ_p is the index of refraction of the plasma, $n(N)$ is the neutral atom number density, ϵ_f is the permittivity of free space, $n(c)$ is the electron number density, ω is the angular frequency of the probing wave, and $1.03\text{x}10^{-23}$ is a constant proportional to polarizability of the argon atom. The change in plasma refractivity ($\Delta\mu_p$) must be measured at two different wavelengths in order to separate the neutral atom number density part of Equation (8) from the electron number density part. This was done by using two laser interferometers with different wavelengths.

Having obtained the electron number density, Gusinow, et al. [10], observed that there was a nonuniform spatial distribution of the neutral-gas density. For the change in the electron number density with time, they used

$$\frac{\partial n(c)}{\partial t} = \nabla \cdot (D_a \nabla n(c)) - \alpha_{CRR}(n(c),T_e)[n(c)]^2 , \qquad (9)$$

where D_a is the ambipolar diffusion coefficient. D_a must be known in order to determine $\alpha_{CRR}(n(c),T_e)$. By an iterative process, Gusinow, et al., could estimate the electron loss due to diffusion as a function of the radial position and with this value calculate the recombination coefficient.

Comparison of $\alpha_{CRR}(n(c),T_e)$ with the values as calculated by Bates, et al. [10], indicated approximate agreement between theory and experiment. However, there are some disadvantages to this method. One must be able to excite and resolve the entire spectrum of resonances in order to measure very small changes in frequency. Also, if the probing frequency is very close to that of the transition frequency of an excited atom, the free electrons and neutral atoms are no longer the main contributors to the refractivity at optical wavelengths. If the polarizability of the neutral atom is dependent on the wavelength then this method is not sufficient to determine n(c), and if the degree of ionization is large and the number of excited atoms is greater than the number of ground-state atoms, then this method is not sufficiently accurate to measure the neutral atom density.

Spectroscopy

The intensity of a spectral line in a plasma can be measured and the intensity converted to the emission coefficient (radiated power per unit volume per unit solid angle) by using the Abel inversion for axisymmetrical sources. Shirai and Tabei [12] have used this method. The total population of each energy level is determined from the above measurements. Then, by using a Boltzmann plot, the electron temperature and electron number density can be calculated from the straight portion of the curve. Using this information, Shirai and Tabei calculated the de-excitation transition probability due to collisions with free electrons from level j to i by

$$n(c)Q(j,i) = \pi e^4 n(c)(g_j/g_i)(8/\pi m_e)^{1/2} \times (kT_e)^{-3/2}\left(\frac{1}{u_i(u_i+1)} - \frac{e^{u_i}-e^{u_{i+1}}}{u_{i+1}(u_{i+1}+1)}\right), \qquad (10)$$

where $u_i = E_i/kT_e$ is the nondimensional excitation energy from level j to i, m_e is the mass of the electron, g_i and g_j are the statistical weights of level i and j, T_e is the electron temperature, and n(c) is the electron number density. Q(j,i) is the cross section of the collision. The recombination coefficient can then be calculated by

$$\alpha_{CRR}(n(c),T_e) = (1/n(c)^2) \sum_{j=m}^{\infty} \sum_{i=1}^{m^*-1} n(N)_j A(j,i)$$

$$+ (1/n(c)^2) \sum_{j=m}^{\infty} \sum_{i=1}^{m^*-1} n(N)_j Q(j,i) \ , \qquad (11)$$

where Q(j,i) is determined by Equation (10). A(j,i) is the spontaneous radiative transition probability.

Since Equation (11) involves an infinite number of terms, compromises must be made in calculating $\alpha_{CRR}(n(c),T_e)$. In fact, all of the above methods are either quite involved or have certain restrictions on the conditions of use. Therefore, another alternative, simpler method has been suggested [13] for determining the recombination coefficient, by measuring the electron number density, using a spectroscopic technique, at two points along the centerline of a partially ionized plasma arcjet. An indepth examination of this spectroscopic technique is the subject of this study and will be described in greater detail in subsequent chapters.

III. THEORETICAL CALCULATIONS

Several attempts have also been made to theoretically determine the recombination coefficient for argon. One of the methods is a solution of the quasi-equilibrium equations for collisional-radiative recombination (CRR) as proposed by Bates, Kingsten, and McWhirter [2]. This method,

descriptive of the physical processes involved, will be discussed in more detail in a subsequent chapter. A second method, proposed by Byron, Stabler, and Bortz [14], uses the principle that under equilibrium conditions there exists a pronounced minimum in the total rate of de-excitation of atoms as a function of the principal quantum number of the excited state. This minimum serves to limit the net rate of three body recombination to the rate of de-excitation of the level at which the minimum occurs. Using this simpler calculational method in the hydrogenic approximation, Wanless [15] obtained recombination coefficients in agreement with the experimental values of Chen [8]. Since Wanless's results agree with the more complex method and cover a wider range of electron temperatures and electron number densities, they are used in this present study for theoretical calculations coupling the gas dynamic and recombination processes.

CHAPTER II

THE RECOMBINATION COEFFICIENT

I. INTRODUCTION

In Chapter I, recombination was defined as any charge-neutralizing encounter between charge carriers of opposite sign moving about in a gas. In this study, because the specie are assumed to be only neutral atoms, free electrons, and positive ions, only electron-ion recombination is considered. In general, the mechanism for change in the electron number density in an ionized gas due to electron-ion recombination can be described statistically [2], or by a complex set of reactions [16]. In the remainder of this chapter the development of the statistical expression, Equation (5),

$$\frac{dn(c)}{dt} = - \alpha_{CRR}(n(c),T_e)[n(c)]^2 , \qquad (5)$$

is discussed.

II. COLLISIONAL-RADIATIVE RECOMBINATION

The initial work on a statistical description of CRR was done by Bates, et al. [2], for optically thin and optically thick plasmas. For the case of an optically thin plasma, they confined their discussion to the recombination

of electrons (denoted by e^-) with bare nuclei (denoted by N^+) of charge Ze (where Z is the level of ionization and e is the charge on an electron) to form hydrogen atoms or hydrogenic ions. Letting p, q, et cetera, denote the principal quantum numbers of the discrete levels and letting c represent the continuum, the number densities of atoms or ions in the indicated levels are denoted by n(p), n(q), et cetera. The number density of free electrons is designated by n(c) and the ions by $n(N^+)$.

Three body recombination into some state p is described by the rate coefficients K(c,p), and the reverse ionizing process by the rate coefficient K(p,c). The collisional excitation or de-excitation process, which can be written as

$$N^+(p) + e^- \rightarrow N^+(q) + e^- , \qquad (12)$$

is described with K(p,q) as the rate coefficient. The radiative recombination rate coefficient is denoted by $\beta(p)$. A(p,q) is used to denote the spontaneous transition probability for the reaction

$$N^+(p) \rightarrow N^+(q) + h\nu . \qquad (13)$$

With the assumptions: (1) that the electronic transitions caused by atom-atom, atom-ion, or ion-ion collisions can be neglected; (2) boundary effects can be neglected; and (3) the plasma is optically thin so that all emitted radiation

escapes the plasma without being absorbed; Bates, et al., were able to express the rate of change of n(p) with time by

$$\frac{dn(p)}{dt} = - n(p)[n(c)H(p) + \bar{A}(p)]$$

$$+ n(c) \sum_{q \neq p} n(q)K(q,p)$$

$$+ \sum_{q>p} n(q)A(q,p)$$

$$+ n(c)^2 X^{-1}[K(c,p) + \beta(p)] \ , \qquad (14)$$

where

$$H(p) = K(p,c) + \sum_{q \neq p} K(p,q) \ ,$$

$$\bar{A}(p) = \sum_{q<p} A(p,q) \ ,$$

and

$$X = n(c)/n(N^+) \ . \qquad (15)$$

Equation (14) is the sum of all the rates that add to or subtract from the number density of atoms in level p.

The ratio

$$\sigma(p) = n(p)/n_E(p) \ , \qquad (16)$$

is introduced where $n_E(p)$ is the number density of hydrogan atoms or hydrogenic ions in level p, which at the electron

temperature T_e is proportional to the free electron number density times the ion number density such that

$$n_E(p) = n(N^+)n(c)p^2\left(\frac{h^2}{2\pi m_e kT_e}\right)^{3/2} e^{I_p/kT_e} , \qquad (17)$$

where I_p is the ionization potential of level p. Under equilibrium conditions, the number of recombining atoms by the process described by Equation (2) will be equal to the number of N^+ being formed by the reverse process. The number of atoms entering level q by the process described by Equation (12) is equal to the number entering level p by the reverse process; therefore,

$$n_E(q)K(q,p) = n_E(p)K(p,q)$$

and

$$n(c)X^{-1}K(c,p) = n_E(p)K(p,c) . \qquad (18)$$

Equation (14) can now be written as

$$\frac{dn(p)}{dt}/n_E(p) = -\sigma(p)[n(c)H(p) + \bar{A}(p)]$$

$$+ n(c)K(p,c) + \sum_{q\neq p}\sigma(q)n(c)K(p,q)$$

$$+ n(c)^2X^{-1}n_E(p)^{-1}\beta(p)$$

$$+ \sum_{q>p}\sigma(q)n_E(q)n_E(p)^{-1}A(q,p) . \qquad (19)$$

Equation (19) gives the increase of the number density of atoms in level p with time. Since there are an infinite number of possible levels, p, the total process is described by an infinite set of coupled differential equations, such as Equation (19), where each equation represents a different quantum level.

Substituting numerical values into Equation (17) gives

$$\frac{n_E(p)}{n(N^+)} = 4.2\text{x}10^{-16}\left(\frac{n(c)p^2}{T_e^{3/2}}\right)e^{I_p/kT_e} . \qquad (20)$$

Since the right side of Equation (20) is multiplied by $4.2\text{x}10^{-16}$, there will be a wide range of T_e's and n(c)'s such that $n_E(p)$ is very much less than n(c) and $n(N^+)$. It follows that for nonequilibrium conditions, which will be for a wider range,

$$n(p) << n(c) \quad (p \neq 1) . \qquad (21)$$

Bates, et al. [2], show that only in the case of extremely dense plasmas is this condition no longer true. Although the original work described by Equation (20) was written for hydrogen, the expression for argon is

$$\frac{n_E(p)}{n(N^+)} = 4.2\text{x}10^{-16}\left(\frac{n(c)}{T_e^{3/2}}\right)\frac{g_p}{g_{i_0}+g_{i_1}e^{-E_1/kT_e}}e^{I_p/kT_e} , \qquad (22)$$

where g_p is the statistical weight of level p for the atom, and g_{i_0} and g_{i_1} are the statistical weights of the levels of energy for the ion. Equation (22) leads to the same conclusion (Equation (21)) as obtained from Equation (20).

In addition to the condition described by Equation (21), the number density of atoms in level p is very much less than the number density of atoms in the ground-state level when the steady state is reached. The relaxation times for the excited levels are very much shorter than the relaxation time for the ground level or for the free electrons. The time rates of change of the population densities for p>1 can be set to zero without causing significant error, Equation (19) determines dn(1)/dt, the rate of disappearance of free charge or

$$\frac{dn(1)}{dt} = - \Gamma n(c) n(N^+) \quad , \tag{23}$$

where Γ is the collisional-radiative decay coefficients [2]. Bates, et al., show that Γ can be written as

$$\Gamma = \alpha_{CRR}(n(c), T_e) - SXn(1)/n(c) \quad , \tag{24}$$

where $\alpha_{CRR}(n(c), T_e)$ is called the collisional-radiative recombination (CRR) coefficient, and S is the collisional-radiative ionization (CRI) coefficient. Using the results of Bates, et al., one can now complete the development of

Equation (5) by the following arguments: Substituting Equation (24) into (23) gives

$$\frac{dn(1)}{dt} = \alpha_{CRR}(n(c),T_e)[n(c)n(N^+)] - SXn(1)n(N^+) \quad , \quad (25)$$

which now defines dn(1)/dt in terms of $\alpha_{CRR}(n(c),T_e)$ and S. In the early part of decay in which n(1) is very low, the term in S may be neglected [2]. This leads to

$$\frac{dn(1)}{dt} = \alpha_{CRR}(n(c),T_e)[n(c)n(N^+)] \quad . \quad (26)$$

If one considers single ionization, then the electron and ion densities are equal and the conservation of heavy particles, as pointed out in Reference [17], can be expressed by the equation

$$\sum n(p) + n(c) = n(N)' \quad , \quad (27)$$

where $n(N)'$ is the total heavy particle density. Taking the derivative with respect to time gives

$$\sum \frac{dn(p)}{dt} + \frac{dn(c)}{dt} = 0 \quad . \quad (28)$$

As noted earlier, the derivatives of the excited levels can be set equal to zero without causing significant error,

$$\frac{dn(l)}{dt} = - \frac{dn(c)}{dt} , \tag{29}$$

which leads to

$$\frac{dn(c)}{dt} = - \alpha_{CRR}(n(c),T_e)[n(c)]^2 , \tag{30}$$

where

$$n(c) = n(N^+) .$$

Thus, in order to determine the recombination coefficient using Equation (30), the electron number density along with its time rate of change is all that is necessary. It should be pointed out that, if feasible, the above approach is significantly simpler than other methods discussed in Chapter I, because of the relatively few measurements necessary and the simplicity of analysis.

CHAPTER III

COLLISIONAL-RADIATIVE RECOMBINATION VERSUS GAS DYNAMICS

I. INTRODUCTION

In the free expansion of a singly ionized argon plasma from an arcjet, the change in the electron number density from one point to another along the centerline is due not only to recombination, but also to the gas dynamic effects. The velocity of the flow can be used in relating time and position, so that in principle, a typical gas dynamic (spatially dependent) description can be used in determining the time rate of changes for the various phenomena. In this chapter, the equations are developed to couple these effects due to the gas dynamics and the electron-ion recombination in order to have a more complete description of the change in electron number density with time. The results from this study will also be discussed.

II. COUPLED COLLISIONAL-RADIATIVE RECOMBINATION WITH GAS DYNAMICS

It has been shown that if the degree of ionization is small, conventional isentropic gas dynamic theory should give a good approximation for the mean plasma

properties from the arcjet [18]. Therefore, [19]

$$\frac{\rho}{\rho_0} = \left(1 + \frac{\gamma-1}{2} M^2\right)^{-\frac{1}{\gamma-1}}, \tag{31}$$

where γ is the ratio of specific heats ($\gamma = 1.67$ for argon), M is the Mach number ($M = v/c_s$ where v is the velocity of the flow and c_s is the speed of sound), ρ is the total mass density at some point downstream of the nozzle, and ρ_0 is the total mass density at stagnation condition. The mass density is directly proportional to the number of particles in the volume; therefore, for two points in the flow

$$\frac{(n(N)+n(N^+))_1}{n_0} = \left(1 + \frac{\gamma-1}{2} M_1^2\right)^{-\frac{1}{\gamma-1}}$$

$$\frac{(n(N)+n(N^+))_2}{n_0} = \left(1 + \frac{\gamma-1}{2} M_2^2\right)^{-\frac{1}{\gamma-1}}, \tag{32}$$

where the n's denote the number densities of the particles. These equations imply

$$\frac{(n(N)+n(N^+))_2}{(n(N)+n(N^+))_1} = \theta^{\frac{1}{\gamma-1}}, \tag{33}$$

where

$$\theta = \left[\frac{1 + \frac{\gamma-1}{2} M_1^2}{1 + \frac{\gamma-1}{2} M_2^2}\right] .$$

Assuming the electrons in the flow of the plasma follow the ions aerodynamically, then the ratio of the electron number density at two points can also be written in terms of the Mach number. This gives

$$\frac{n(c)_2}{n(c)_1} = \theta^{\frac{1}{\gamma-1}} . \tag{34}$$

However, the electron number density is further depleted by the effects of recombination. Thus, an additional term must be added to Equation (34) in order to account for this. This leads to

$$\frac{n(c)_2}{n(c)_1} = \theta^{\frac{1}{\gamma-1}} + \frac{1}{n(c)_1} \int_{t_1}^{t_2} \left(\frac{dn(c)}{dt}\right)_{CRR} dt , \tag{35}$$

where the additional term is the contribution of the recombination process. The

$$\left(\frac{dn(c)}{dt}\right)_{CRR}$$

is the change in the electron number density with respect to time due to collisional-radiative recombination. Using

the definition of

$$\left(\frac{dn(c)}{dt}\right)_{CRR}$$

in Equation (30) gives

$$\frac{n(c)_2}{n(c)_1} = \theta^{\frac{1}{\gamma-1}} + \frac{1}{n(c)_1}\int_{t_1}^{t_2} - \alpha_{CRR}(n(c),T_e)\,[n(c)_2]^2\,dt \quad . \quad (36)$$

Assuming that conditions at position one are constant as viewed from position two, the derivative of $n(c)_2$ is

$$\frac{dn(c)_2}{dt} = - n(c)_1 \left(1 + \frac{\gamma-1}{2} M_1^2\right)^{\frac{1}{\gamma-1}}$$

$$\left(1 + \frac{\gamma-1}{2} M_2^2\right)^{- \frac{\gamma}{\gamma-1}} M_2 \frac{dM_2}{dt}$$

$$- \alpha_{CRR}(n(c),T_e)\,[n(c)_2]^2 \quad . \quad (37)$$

Thus, the rate of change of n(c) due to gas dynamic effect is

$$\left(\frac{dn(c)}{dt}\right)_{GD} = - n(c)_1\, \phi M^2 \frac{dM_2}{dx_2} \frac{dx_2}{dt} \quad , \quad (38)$$

where

$$\phi = \left(1 + \frac{\gamma-1}{2} M_1^2\right)^{\frac{1}{\gamma-1}} \Big/ \left(1 + \frac{\gamma-1}{2} M_2^2\right)^{\frac{\gamma}{\gamma-1}} ,$$

and, as before, the rate of change due to recombination is

$$\left(\frac{dn(c)}{dt}\right)_{CRR} = - \alpha_{CRR}(n(c), T_e)\,[n(c)_2]^2 . \qquad (39)$$

In order to effect a solution of Equations (38) and (39), so that a comparison of the two rates can be made, M_2 , dM_2/dx_2 , and dx_2/dt must be determined. Since White [20] has shown that his experimentally determined Mach number distribution is in good agreement with the Ashkenas-Sherman model [21] for the Mach number distribution on the plume centerline, this model was used in determining M_2 and dM_2/dx_2 along the centerline. From this model

$$M_2 = A'\left(\frac{x_2-x_0}{D}\right)^{\gamma-1} - \frac{1}{2}\left(\frac{\gamma+1}{\gamma-1}\right) \Big/ A'\left(\frac{x_2-x_0}{D}\right)^{\gamma-1} + C\left(\frac{x_2-x_0}{D}\right)^{-3(\gamma-1)} , \qquad (40)$$

where A', C, and x_0 are empirical constants which depend on γ. The distance from the exit plane is denoted by x_2. A value for x_0 is found by projecting streamlines back to the axis. Then values of M and x/D from the characteristics

solution can be inserted into Equation (40), and a constant value for A' and C can be determined. Using the final values in Equation (40), Ashkenas and Sherman could reproduce the Mach numbers from the characteristics solution with a deviation of about $\pm 0.5\%$. For a γ of 1.67, Ashkenas and Sherman determined A' to be 3.26, C to be 0.31, and x_0/D to be 0.075 (D being the diameter of the nozzle).

Equation (40) can be used in obtaining dM_2/dx_2, which is

$$\frac{dM_2}{dx_2} = \left(\frac{A'(\gamma-1)}{D}\right)(S')^{\gamma-2} + \frac{\gamma+1}{2A'D(S')^{\gamma}} - 3(\gamma-1)\frac{C}{D}(S')^{-3\gamma+2} , \qquad (41)$$

where

$$S' = (x_2 - x_0) / D .$$

The velocity of the flow at x_2 can be written as

$$\frac{dx_2}{dt} = v_2 = M_2 c_s , \qquad (42)$$

where c_s is the speed of sound. Using the perfect gas relation for c_s gives

$$\frac{dx_2}{dt} = M_2(\gamma R T_{g_2})^{1/2} , \qquad (43)$$

where

$$T_{g_2} = T_0 \; / \; (1 + \frac{\gamma-1}{2} M_2^2) \; , \qquad (44)$$

T_0 is the stagnation temperature, R is the gas constant (R is 2.08×10^6 ergs/(g mole)/°K for argon), and T_{g_2} is gas temperature at x_2.

In order to solve Equations (38) and (39), an initial $(x/D)_0$, T_{g_0} , $n(c)_0$, and time must be specified. With these initial values Equation (38) can be solved by using Equations (40-44). However, before solving Equation (39), the electron number density must be determined from Equation (35), but the recombination coefficient must be determined in order to solve Equation (35).

An existing program for a helium plasma [22] that obtains a solution to Equations (38) and (39) was modified for argon. One of the modifications was the determination of the recombination coefficient. As was noted in Chapter I, a great deal of work has been done in determining the recombination coefficient for argon. One of many investigators is Wanless [15], who has calculated a set of recombination coefficients for argon using the bottle neck principle, which states that the recombination rate can be defined as the total de-excitation rate past the energy level for which the total de-excitation rate is a minimum. Wanless obtained satisfactory agreement with the experimental and theoretical determinations of Chen [8] for the

recombination coefficient. Therefore, Wanless's set of calculated recombination coefficients is used in the above mentioned computer program for solving Equations (35) and (39). Wanless calculated recombination coefficients for electron number densities ranging from $1x10^{10}$ $1/cm^3$ to $1x10^{16}$ $1/cm^3$ and for electron temperature of 2000°K to 16,000°K. In order to expand the study to higher electron number densities used in some of the studies included herein, Wanless's data were extrapolated to include electron number densities of $1x10^{18}$ $1/cm^3$ and electron temperature of 20,000°K. Results of these extrapolations and the values used in this study are shown in Table I. The extrapolation procedure is expected to introduce values of the recombination coefficient that are not completely accurate.

Since the recombination coefficient is a function of n(c) and the electron temperature, the recombination coefficient can be interpolated from the expanded set of recombination coefficients from Wanless if the corresponding n(c) and electron temperature are known. Since the level of ionization is specified as an initial condition, n(c) is known. Thus, a method for determining the electron temperature is required. This was accomplished, when the program was originally written for helium, by assuming an analytic form for the electron temperature [22],

$$T_e = (2544.8)t^{-0.0995}, \qquad (45)$$

TABLE I

Extrapolated Values for the Recombination Coefficient from Wanless's Data

T_e (°K)	n(c) ($1/cm^3$)	$\alpha_{CRR}(n(c), T_e)$ (cm^3/sec)
2,000	$1x10^{17}$	$1.6x10^{-5}$
2,000	$1x10^{18}$	$1.6x10^{-5}$
4,000	$1x10^{17}$	$5.4x10^{-7}$
4,000	$1x10^{18}$	$7.6x10^{-6}$
8,000	$1x10^{17}$	$5.9x10^{-10}$
8,000	$1x10^{18}$	$9.4x10^{-10}$
10,000	$1x10^{17}$	$8.9x10^{-11}$
10,000	$1x10^{18}$	$1.2x10^{-10}$
14,000	$1x10^{17}$	$1.4x10^{-11}$
14,000	$1x10^{18}$	$1.6x10^{-11}$
16,000	$1x10^{17}$	$7.8x10^{-12}$
16,000	$1x10^{18}$	$8.2x10^{-12}$
20,000	$1x10^{10}$	$4.2x10^{-13}$
20,000	$1x10^{11}$	$4.5x10^{-13}$
20,000	$1x10^{12}$	$5.4x10^{-13}$
20,000	$1x10^{13}$	$7.4x10^{-13}$
20,000	$1x10^{14}$	$1.4x10^{-12}$
20,000	$1x10^{15}$	$1.4x10^{-12}$
20,000	$1x10^{16}$	$2.2x10^{-12}$
20,000	$1x10^{17}$	$3.8x10^{-12}$
20,000	$1x10^{18}$	$3.5x10^{-12}$

where t is the time elapsed from the initial time. Additionally, investigators at Arnold Engineering Development Center (AEDC) [23] have made measurements of the electron temperature as a function of x/D in the plume of an argon arcjet, and T_e can be determined from this work in the interval $0.0 \leq x/D \leq 12.0$ (see Figure 1). Both Equation (45) and the set of electron temperatures from Reference [23] were used in this modified program. For Equation (45) the average elapsed time is determined by integrating $x/(dx/dt)$ (using Simpson's rule). The value of x is obtained by stepping from $(x/D)_0$ in intervals of $\Delta(x/D)$.

Once the electron temperature is determined, $\alpha_{CRR}(n(c),T_e)$ is obtained from data expanded from Wanless, as previously discussed. Thus, the n(c) calculated from Equation (35) is used in solving Equation (39) for the time rate of change in n(c) due to recombination alone.

III. INITIAL CONDITIONS

The initial conditions required to obtain the solution to the coupled equations are the gas temperature, electron number density, and the starting position in the plume ($(x/D)_0$). Since the Ashkenas-Sherman model for Mach number does not give reliable results for $x/D < 1$, this value was used for $(x/D)_0$. For the purpose of electron temperature determinations (for example, Equation (45)), an initial time of 1×10^{-9} sec was associated with this $(x/D)_0$.

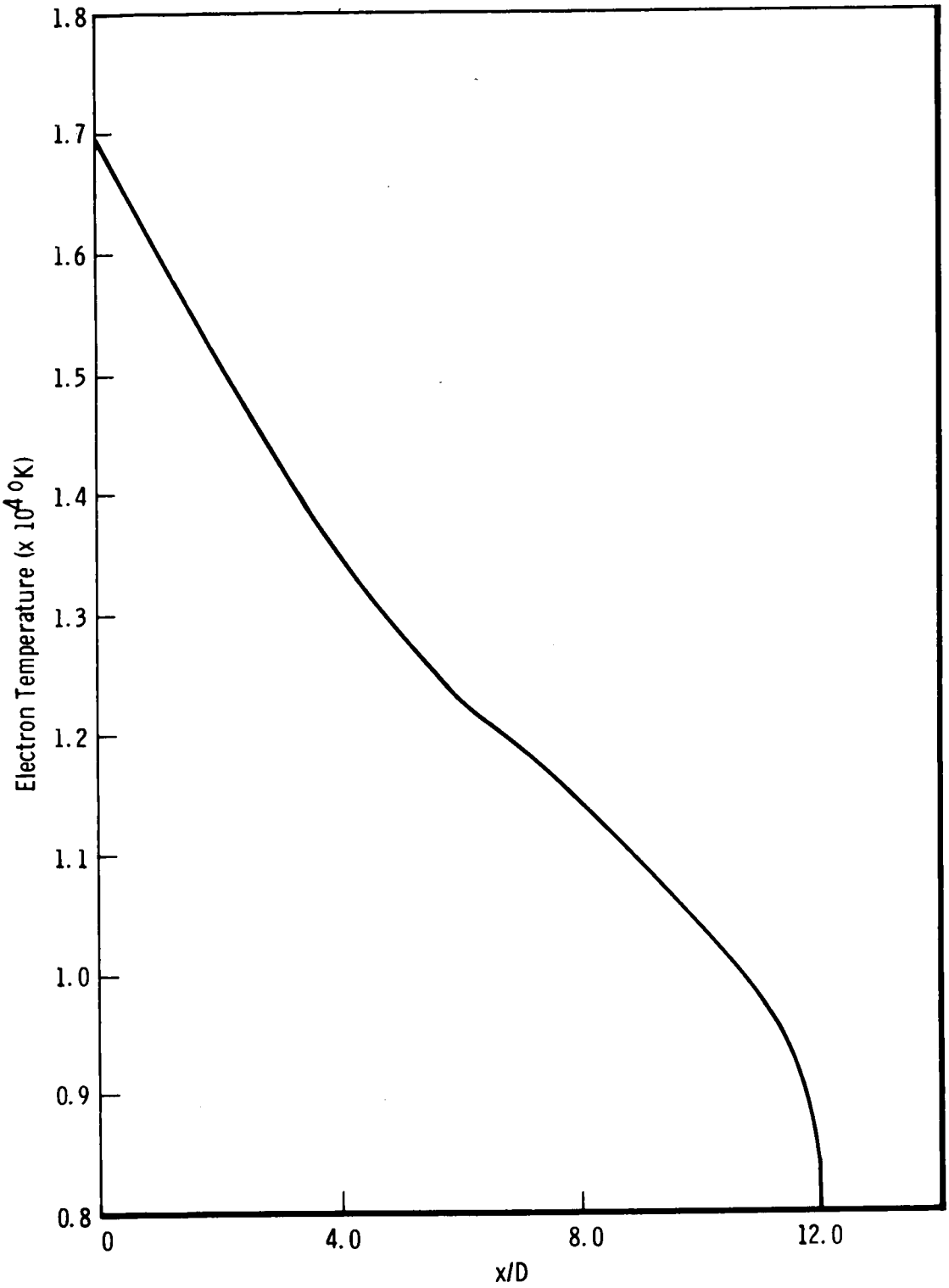

Figure 1. Electron temperature variation on the axis of an expanding argon plasma jet; initial electron temperature of 17,000°K [23].

The gas temperature at this position in the plume was determined from stagnation conditions for the arcjet which were consistent with previous determinations [24, 25]. The initial electron number density chosen for these calculations was initially based also upon previous observations (typically, 1% ionization of stagnation atom density). Analysis of these results, described below, prompted calculations at the higher initial electron number densities listed in Table II. It should be pointed out that the electron number densities listed in Table II are in effect a stagnation condition, whereas the calculations were actually started at $(x/D)_0 = 1.0$. Thus, although some of the values of $n(c)_0$ listed in Table II are out of the range of Table I, page 29, the n(c) at $(x/D)_0 = 1.0$ are within the range of Table I because of the expansion.

IV. RESULTS

The initial conditions listed in Table II were used in the coupled recombination and gas dynamics (CRR-GD) program to determine the rate of change in the electron number density due to the recombination and the gas dynamics. The results of some of the calculations are shown in Figures 2, 3, and 4. The two curves plotted are the rates due to the gas dynamics and the recombination mechanisms. The electron temperature as a function of time was

TABLE II

Initial Values of Gas Temperature and Electron Number Density for the Collisional-Radiative Recombination-Gas Dynamic Program

T_{g_0} (°K)	$n(c)_0$ ($1/cm^3$)
1365	3.31×10^{14}
2715	8.27×10^{13}
2222	4.52×10^{14}
1365	3.31×10^{16}
2715	8.27×10^{15}
2715	3.31×10^{15}
2715	4.52×10^{16}
2715	3.45×10^{17}
2715	8.27×10^{17}
2715	5.00×10^{18}

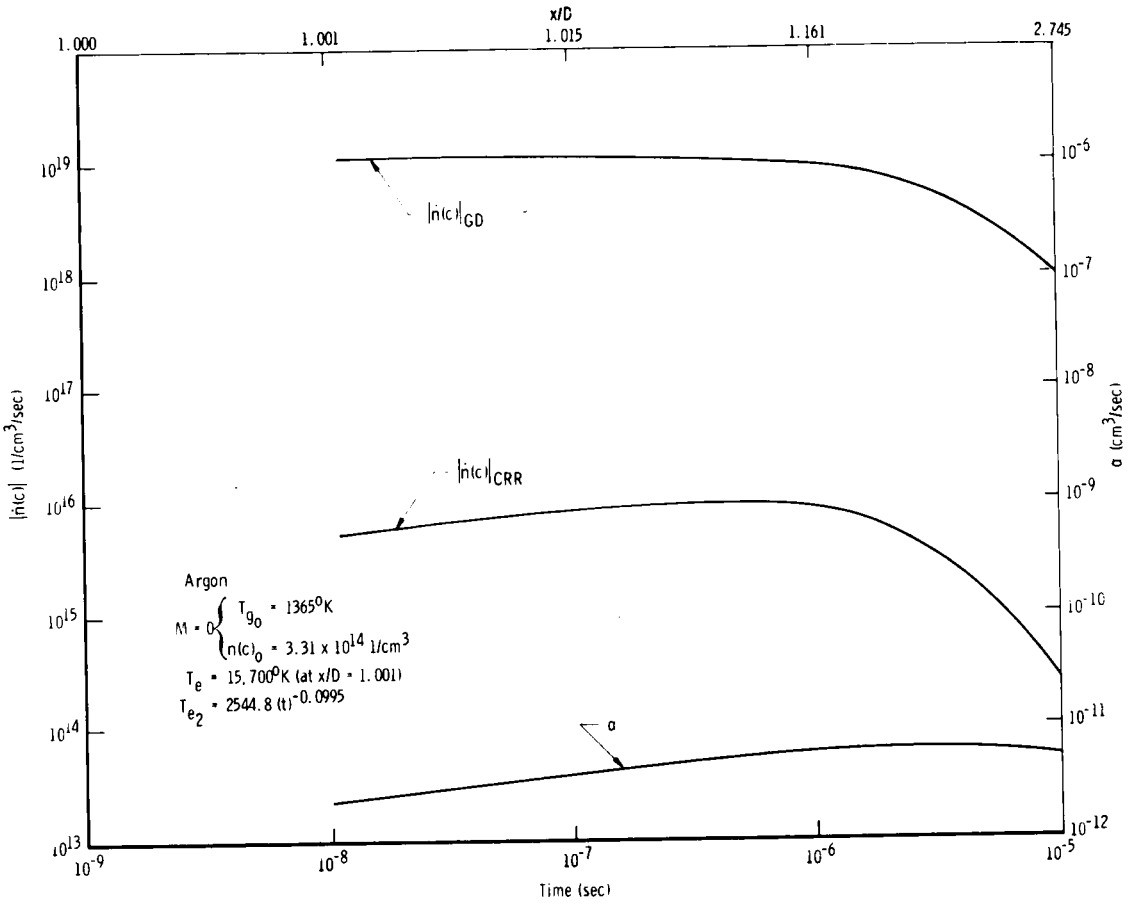

Figure 2. Collisional-radiative recombination rate and gas dynamic rate versus time; initial gas temperature of 1365°K, initial electron number density of 3.31×10^{14} 1/cm^3, and electron temperature (at x/D = 1.001) of 15,700°K.

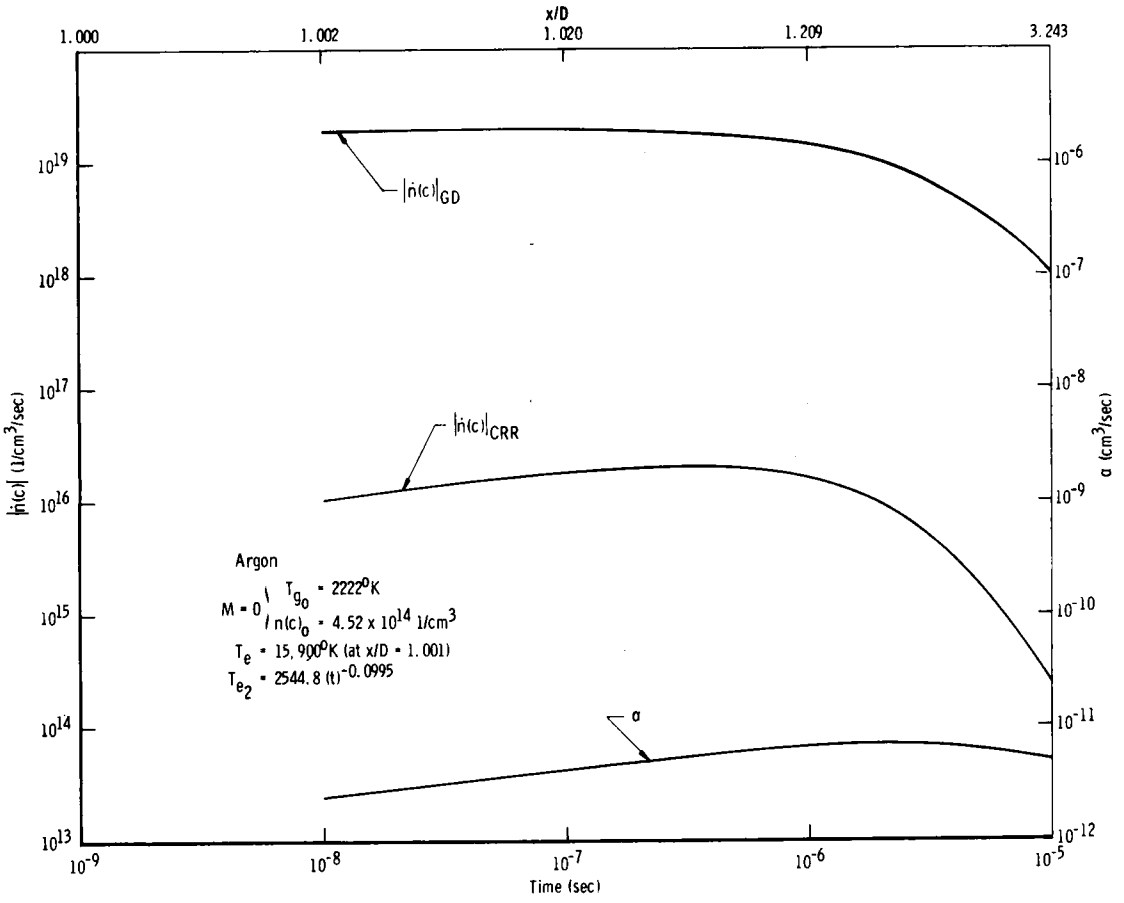

Figure 3. Collisional-radiative recombination rate and gas dynamic rate versus time; initial gas temperature of 2222°K, initial electron number density of 4.52×10^{14} 1/cm^3, and electron temperature (at x/D = 1.001) of 15,900°K.

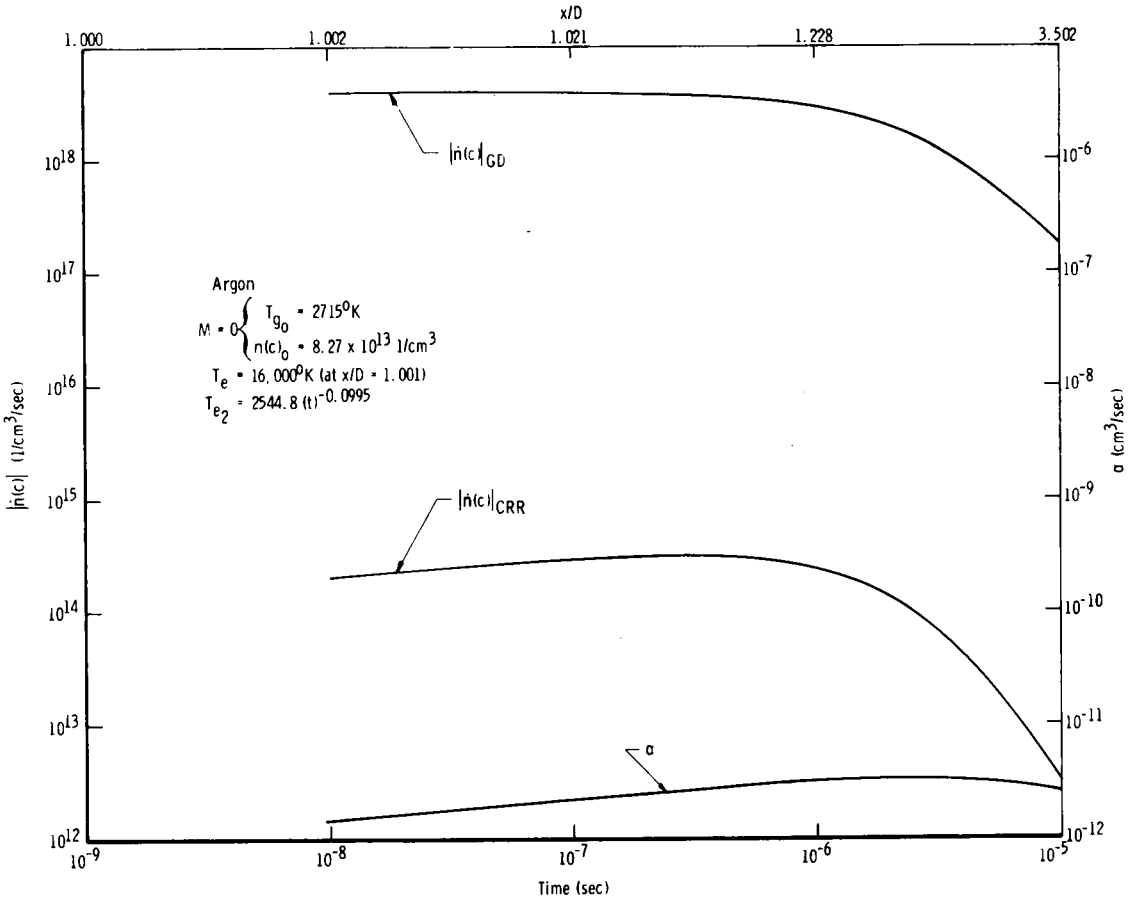

Figure 4. Collisional-radiative recombination rate and gas dynamic rate versus time; initial gas temperature of 2715°K, initial electron number density of 8.27×10^{13} 1/cm^3, and electron temperature (at x/D = 1.001) of 16,000°K.

determined by Equation (45) in these calculations. Also, a plot of $\alpha_{CRR}(n(c),T_e)$ versus time is shown in each figure.

The results shown in Figure 2 are for an expansion whose initial gas temperature is 1365°K and initial electron number density is 3.31×10^{14} $1/cm^3$, while for Figure 3 the initial gas temperature is 2222°K and the electron number density is 4.52×10^{14} $1/cm^3$. In Figure 4 the initial gas temperature is 2715°K and the electron number density is 8.27×10^{13} $1/cm^3$. The results show that, for all these conditions, the gas dynamic rate is dominant over the CRR rate by at least three orders of magnitude, making CRR a relatively insignificant contribution.

It was observed that increasing the initial electron number density reduces the difference in the two rates. This is illustrated in Figure 5, for an initial gas temperature of 1365°K and an electron number density of 3.31×10^{16} $1/cm^3$, which is 100% ionization at these conditions. Also plotted in Figure 5, for comparison purposes, is the total rate of decay of the electron number density. As is seen on Figure 5, even at this condition, the collisional-radiative recombination rate is never above the gas dynamic rate, although they are equal for a small interval of time.

Noting that generally increasing the electron number density caused the recombination rate to increase, similar calculations were made for a plasma expansion at an

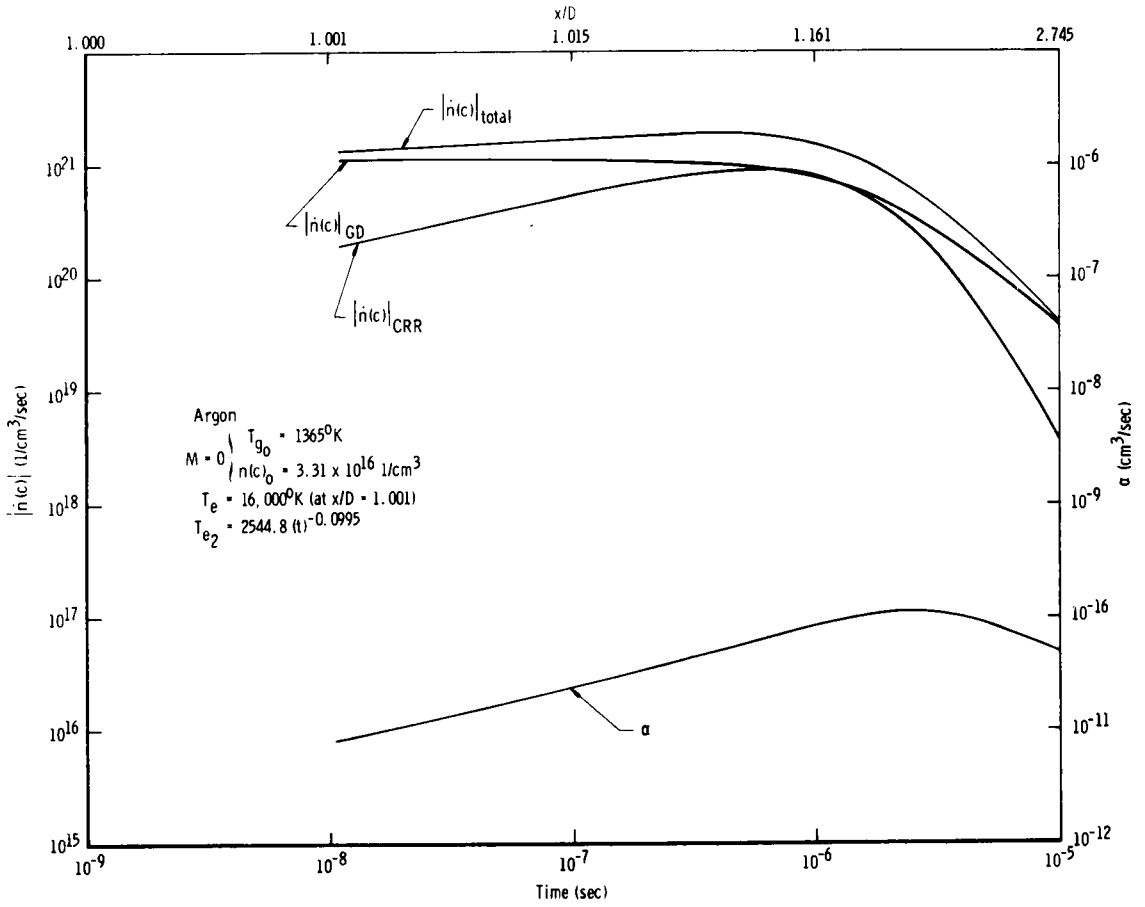

Figure 5. Collisional-radiative recombination rate and gas dynamic rate versus time; initial gas temperature of 1365°K, initial electron number density of 3.31 x 10^{16} 1/cm^3, and electron temperature (at x/D = 1.001) of 16,000°K.

initial gas temperature of 2715°K and electron number density of 3.45×10^{17} $1/cm^3$. These results are shown in Figure 6. At this electron number density the recombination rate does dominate the gas dynamic rate in the interval 1×10^{-8} sec $\leq t \leq 3 \times 10^{-6}$ sec. However, for $t > 3 \times 10^{-6}$ sec, corresponding to approximately $x/D > 2$, the gas dynamic rate is the dominant feature of the decay and remains so. It should be noted that this electron number density is quite high practically, corresponding approximately to 100% single ionization of an argon gas at 3000°K and 76 torr. Hence, for cases of immediate practical interest, one concludes that the CRR rate will dominate the total rate.

For the purpose of further exploration of comparisons of the GD and CRR rates, the ratio of the CRR rate to the GD rate versus x/D is informative. When this ratio is one the CRR rate will be equal to the GD rate and when the ratio is greater than one the CRR rate will be larger than the GD rate. Therefore, for recombination to be observable, the plot of the ratio must be greater than one. Figure 7 (still using Equation (45) for determining T_e) presents the results of calculating the ratio of the two rates for various initial electron number densities for an initial gas temperature of 2715°K. For an initial electron number density of 5×10^{18} $1/cm^3$ the curve starts with the ratio greater than one, but at an x/D of approximately 1.80 the ratio becomes less than one and the GD rate is greater

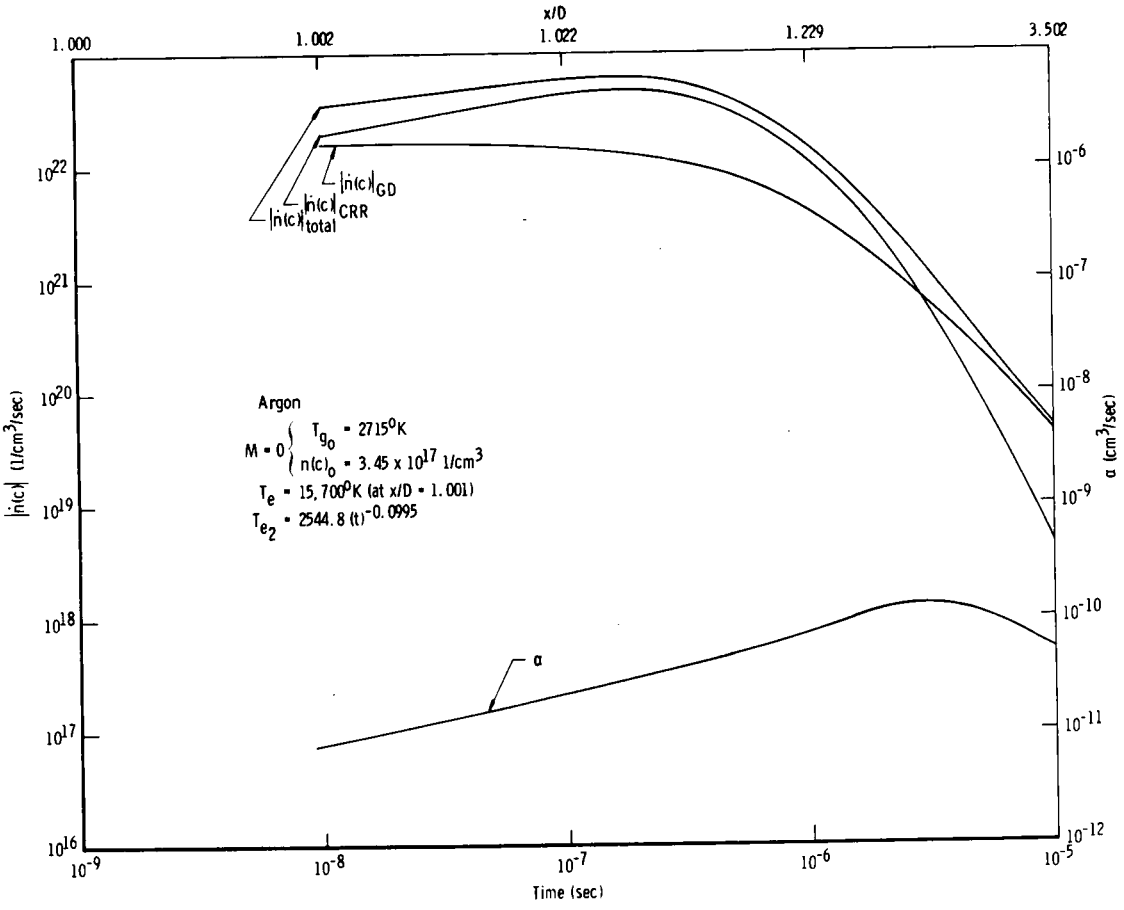

Figure 6. Collisional-radiative recombination rate and gas dynamic rate versus time; initial gas temperature of 2715°K, initial electron number density of 3.45x10^{17} 1/cm^3, and electron temperature (at x/D = 1.001) of 15,700°K.

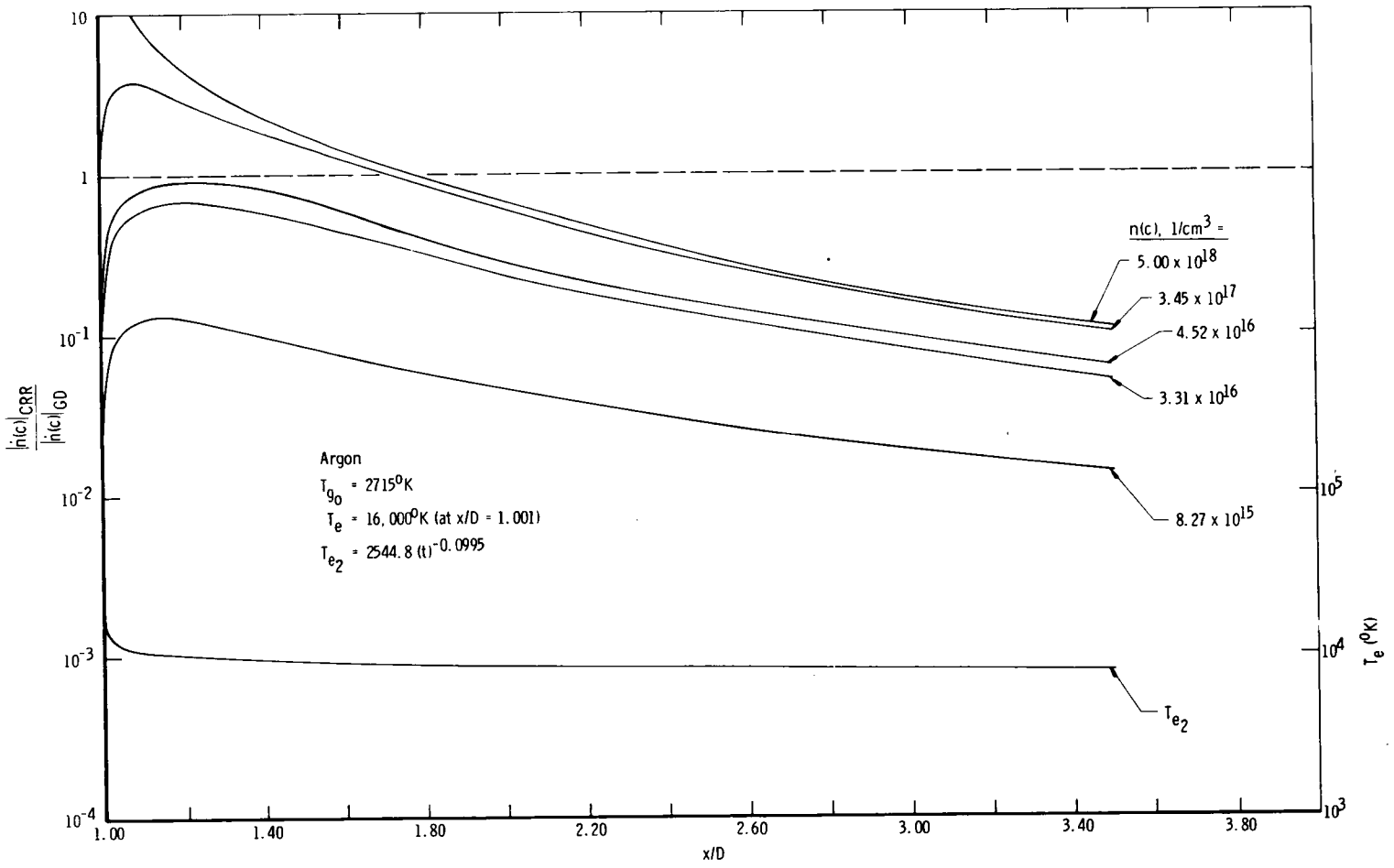

Figure 7. Ratio of collisional-radiative recombination rate to gas dynamic rate; initial gas temperature at 2715°K and electron temperature (at x/D = 1.001) of 16,000°K (using Equation (45) for determining T_e).

than the CRR rate. For an electron number density less than approximately 5×10^{16} $1/cm^3$ the ratio is never greater than one.

Figure 8 illustrates the results of the calculations for the ratio of the two rates versus x/D where the electron temperature is determined from a table of values that is taken from Reference [23]. A plot of these data is shown in Figure 1, page 31. The initial gas temperature was 2715°K as was the case for the results shown in Figure 7. For an initial electron number density of 5×10^{18} $1/cm^3$ the ratio starts out greater than one, but falls off rapidly to less than one at an x/D less than 1.6. For the other initial electron number densities used the ratio was never greater than one. Thus, as with the analytical electron temperature gradient, the rate of change of electron number density due to the gas dynamic effects will dominate the rate due to CRR, even at unrealistically high number densities.

V. ELECTRON NUMBER DENSITY

From Equations (38) and (39) the ratio of the CRR rate to the GD rate can be written as

$$\frac{dn(c)/dt)_{CRR}}{dn(c)/dt)_{GD}} = \frac{\alpha_{CRR}(n(c),T_e)\,[n(c)_2]^2}{n(c)_1\ \phi M_2\ dM_2/dx_2\ dx_2/dt}\ , \qquad (46)$$

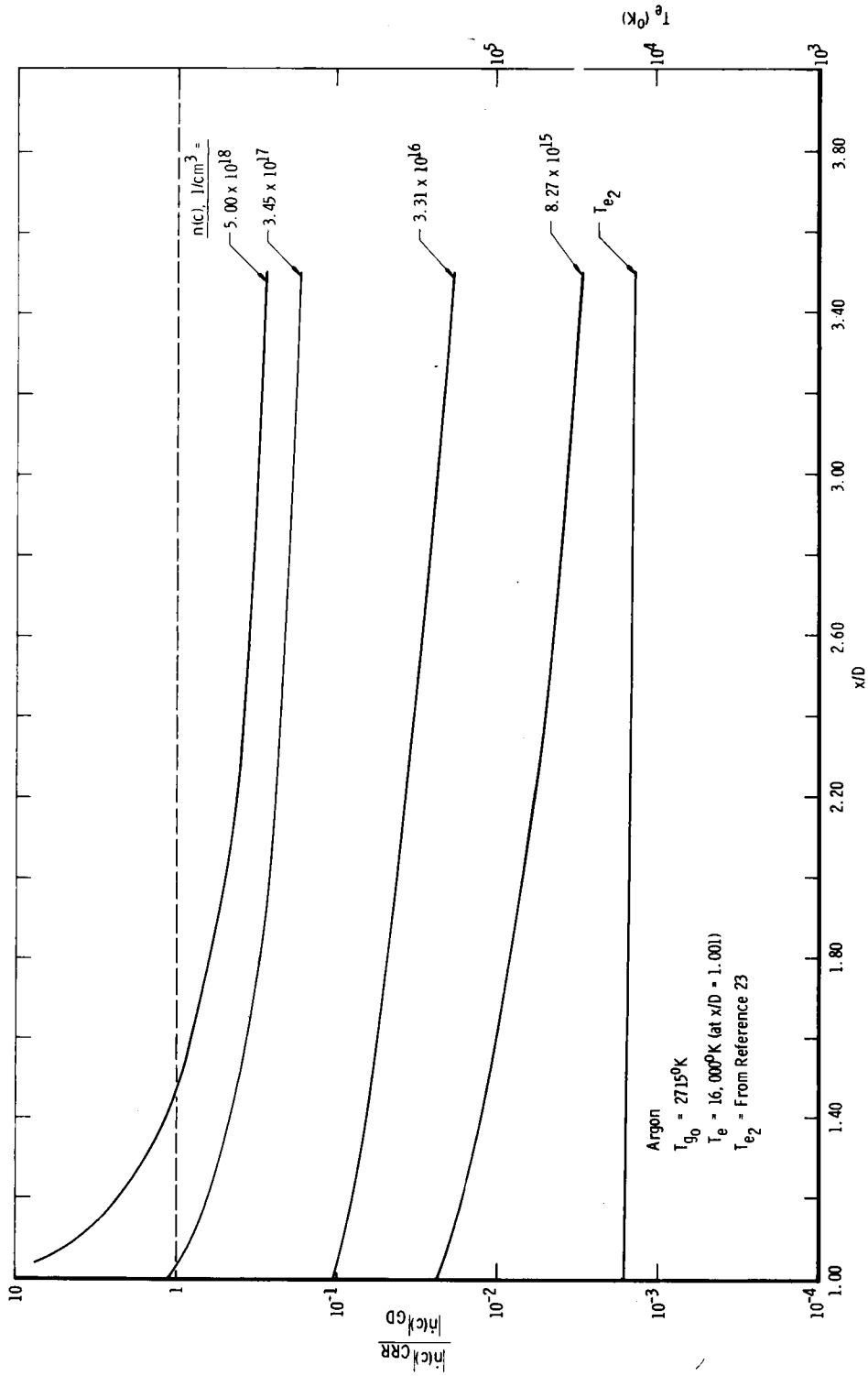

Figure 8. Ratio of collisional-radiative recombination rate to gas dynamic rate; initial gas temperature of 2715°K and electron temperature (at x/D = 1.001) of 16,000°K (using Reference [23] for determining T_e).

where all the symbols have the same meaning as given earlier. When the ratio is one the CRR rate is equal to the GD rate. If the ratio is one then Equation (46) can be rewritten as

$$n(c)_2 = \left(\frac{n(c)_1 \, M_2 \phi \, dM_2/dx_2 \, dx_2/dt}{\alpha_{CRR}(n(c), T_e)}\right)^{1/2}, \qquad (47)$$

which is the electron number density when the two rates are equal. Thus, by calculating the electron number density when the two rates are equal, the electron number density required for the CRR rate to dominate the GD rate can be estimated.

Figure 9 illustrates the results from this calculation for an initial gas temperature of 2715°K and an initial electron number density of 5×10^{18} $1/cm^3$. The $n(c)'$ is the electron number density as calculated from Equation (47) where the ratio is assumed to be one. The n(c) curve is the electron number density with the decay proceeding normally. For the CRR rate to dominate, the GD rate n(c) must be greater than $n(c)'$. As can be seen on Figure 9, this condition is not met except at the very earliest positions in the flow. Thus, one is again forced to the conclusion that the gas dynamic rate of change of the free electron number density will dominate the collisional-radiative recombination rate for typical physically obtainable arcjet plumes.

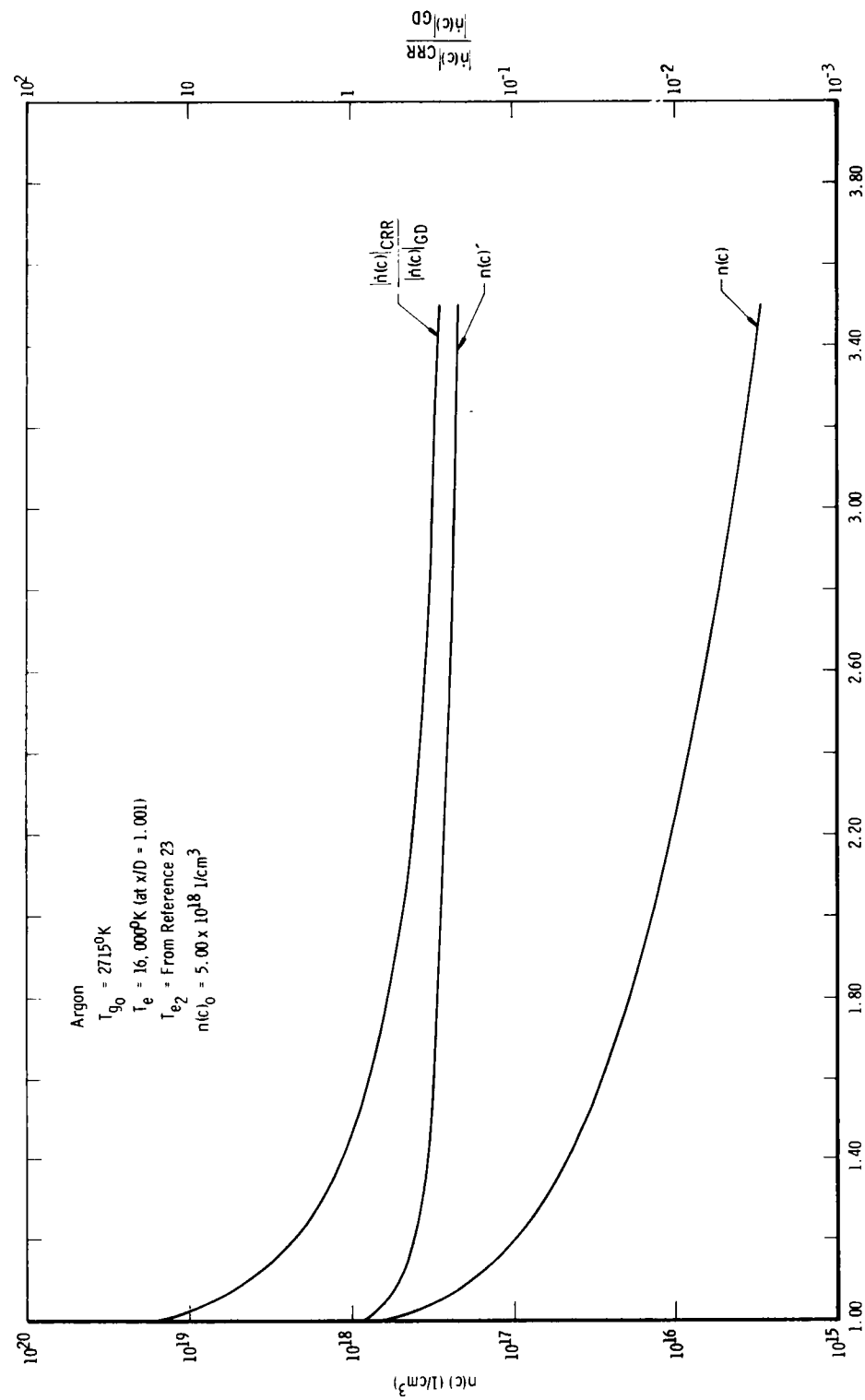

Figure 9. Electron number density and electron number density when collisional-radiative recombination rate equals the gas dynamic rate versus x/D.

CHAPTER IV

EXPERIMENTAL DATA

I. INTRODUCTION

At Arnold Engineering Development Center [18, 23, 26] the argon arcjet is being used in continuing research work. In the course of the investigation presented herein, heretofore unpublished data have been taken for the purpose of temperature determinations which can be used for comparisons with the conclusions of the previous chapters. In this chapter the procedures for obtaining the experimental data and the analysis will be discussed.

II. APPARATUS AND PROCEDURE

The plasma jet used is of the Gerdien type and one model has been described in detail [26]. In the present study the plasma jet and other apparatus are similar to that described in Reference [27]. Briefly, the arcjet consists of a hollow body into which the working gas is introduced. The plasma is produced in the arc region between a coaxial water cooled tungsten cathode and a water cooled constant area copper nozzle anode. The plasma exhausts through this nozzle into the test cell. The pressure in the test cell is maintained by two large mechanical vacuum pumps. A quartz window is mounted in the test cell for spectroscopic

observations. In this study the arcjet nozzle had a diameter of 0.635 cm. Figure 10 is a schematic representation of the test apparatus which is not to scale.

The chamber and lines were pumped before arcjet operation in order to assure minimum contamination. The argon gas supply was from a set of K-bottles of 99.9% purity (with oxygen 1 PPM, nitrogen 1 PPM, hydrogen 1 PPM, and moisture 1 PPM) and was supplied to the gas lines through a regulator adjusted to maintain a line pressure of 5750 torr. The power supply to the arcjet was a motor generator providing an open line voltage of 85 volts. The argon gas was introduced into the arcjet chamber and the plasma jet was started with an RF discharge of short duration which is used to break down the gas and then is shut off after the arc is started. Stable operating conditions were as follows:

1. Chamber pressure : 142.2 torr.
2. Gas flow : 3.0 gm/sec.
3. Operating amperage: 200 amps.
4. Operating voltage : 25 volts.
5. Cell pressure : 0.4 torr.

A one-meter Jarrell-Ash spectrometer was placed so that the entrance slit (slit width of 18μ) was aligned with the centerline of the nozzle and both sides of the plume were scanned. In order to measure the intensities of lines throughout the radial extent of the plasma, the spectrometer field of view was scanned from the centerline of the plasma.

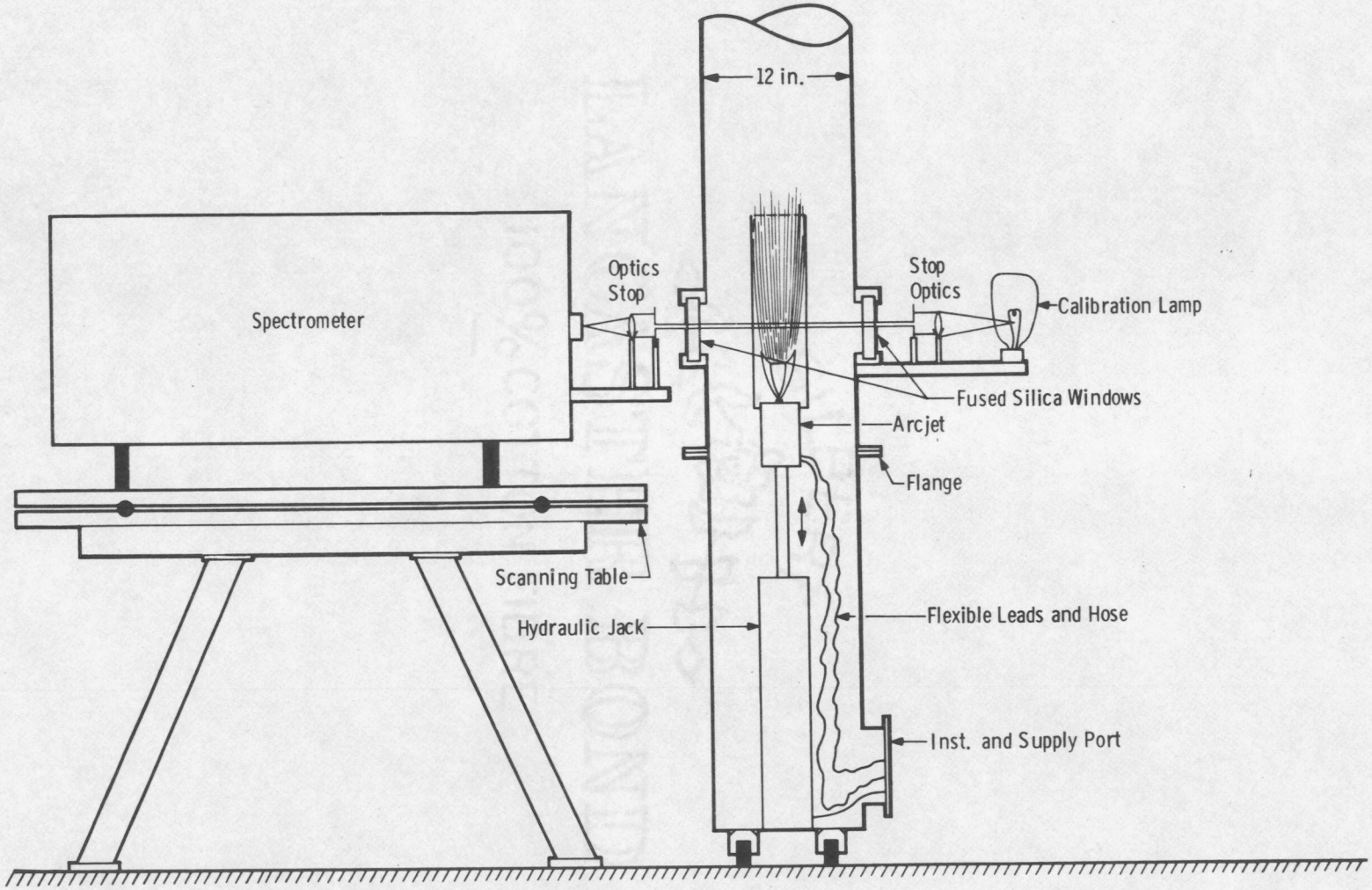

Figure 10. Plasma jet and test cell schematic [27].

This was accomplished by an optical system consisting of a converging lens with a focal length of 30.48 cm and a plane mirror. The mirror was rotated at an angular velocity of 72°/minute so as to provide the scan of the field of view. The lens focused the light from the plasma onto the slit of the spectrometer. The detector was an RCA IP28 photomultiplier tube which was connected to a Philbrick (model P2) amplifier. The gain on the amplifier was set at 100. The amplifier was connected to a Hewlett-Packard x-y recorder. The linear motion of the pen along the paper was at a rate of 4.0 cm/sec. In Figure 11 is a block diagram of these electronics.

After each scan the arcjet was lowered 0.635 cm and another scan was made. This procedure was continued until measurements of the intensity (radiated power per unit area per unit solid angle) of the selected spectral lines had been made at 0.635 cm intervals in the region of study. The 4158 Å spectral line and the 6032 Å spectral line were selected because reliable transition probabilities were available [13].

A calibrated tungsten filament lamp was used for an *in situ* calibration of the spectrometer and optical system. In Table III is a list of the calibration scale factors for the two wavelengths (4158 Å and 6032 Å) that were used in this study. With these calibration values (which take into account the difference in using the

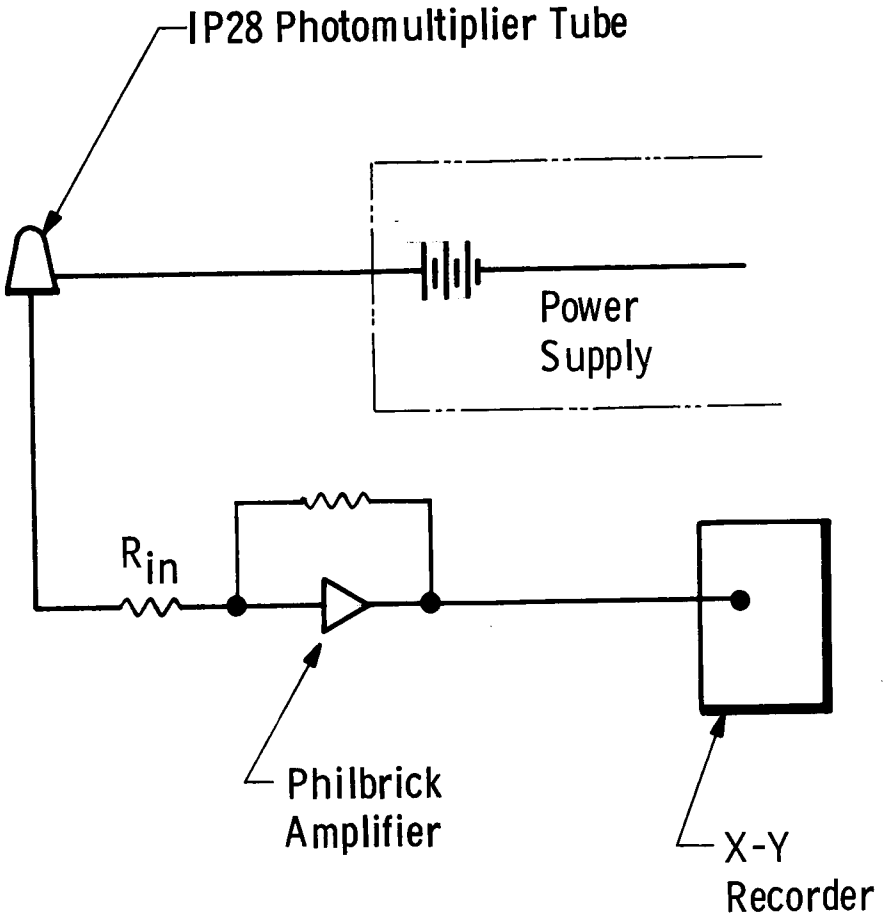

Figure 11. Electronic sketch.

TABLE III

Calibration Factors for Raw Data (Intensity)

x/D	c' (watts/ster. cm^2/div.) 4158 Å	6032 Å
3.0	7.12×10^{-6}	3.73×10^{-6}
4.0	7.12×10^{-6}	3.73×10^{-6}
5.0	2.85×10^{-6}	1.87×10^{-6}

tungsten source as compared to the plasma source) the numbers read from the traces on the x-y recorder can be given physically meaningful units. Thus, the raw data are related to a true intensity of watts/ster. cm^2.

Figures 12 through 17 are traces from the x-y recorder of the intensities (arbitrary units) for both the 4158 Å line and the 6032 Å line that were used in this study. The plume was scanned at least twice for each spectral line to verify arcjet stability and symmetry. The center of each peak corresponds to the location of the centerline of the plume and the scans were examined for repeatability and symmetry. In each case symmetry was satisfactory and the peak height was repeatable within 5%. These variations were judged to be insignificant and intensity data, as a function of distance from the centerline, were obtained from the right side of one scan only. These data were then converted to intensity units by the appropriate calibration.

III. ANALYSIS

The above line intensity measurements were used to obtain the local emission coefficients (radiated power per unit volume per unit solid angle) by use of the Abel inversion [28]. A program [22] that was written for this inversion of the data from a cylindrically symmetric source was used to calculate the emission coefficient. Figure 18

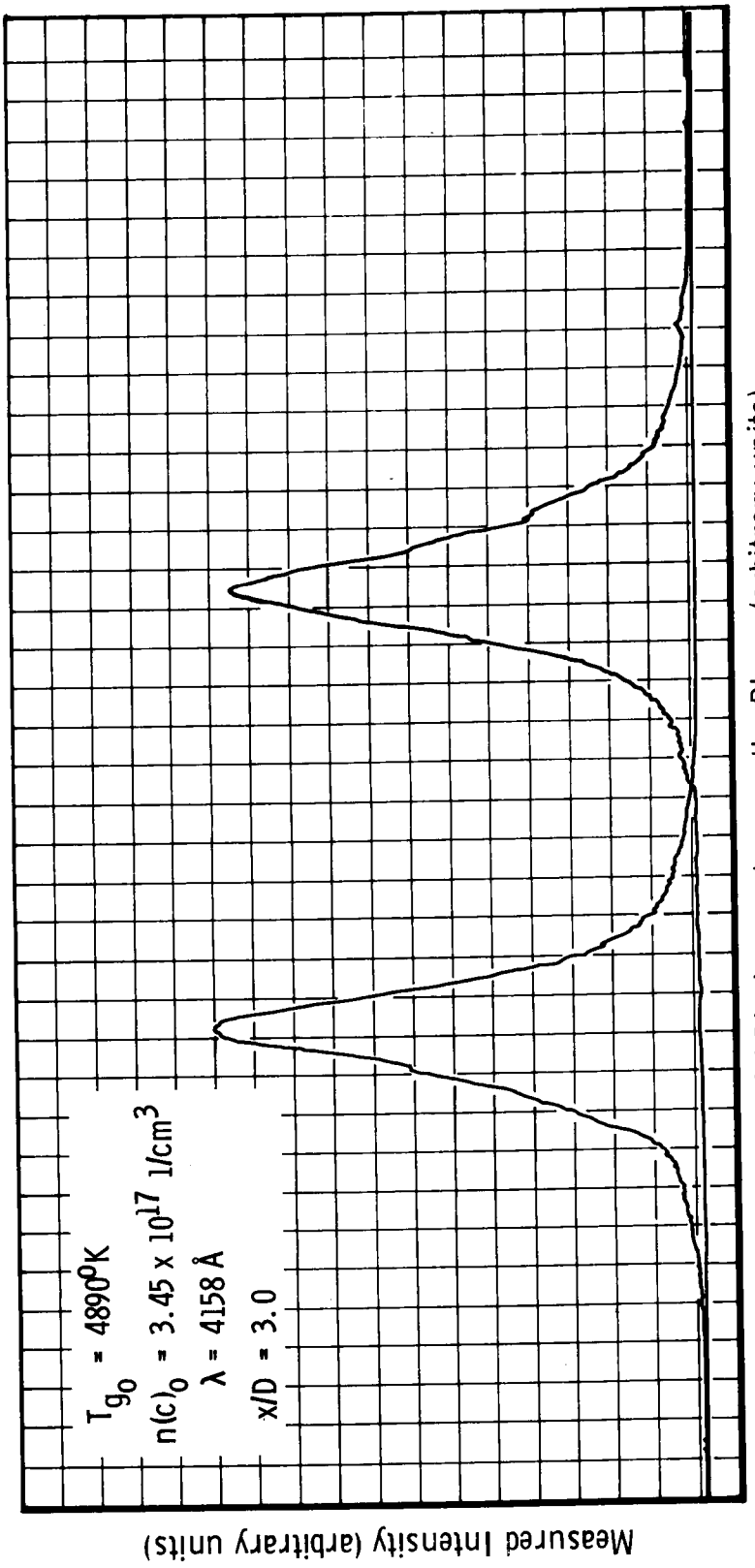

Figure 12. Raw data (intensity) scans for a wavelength of 4158 Å at a position (x/D) of 3.0.

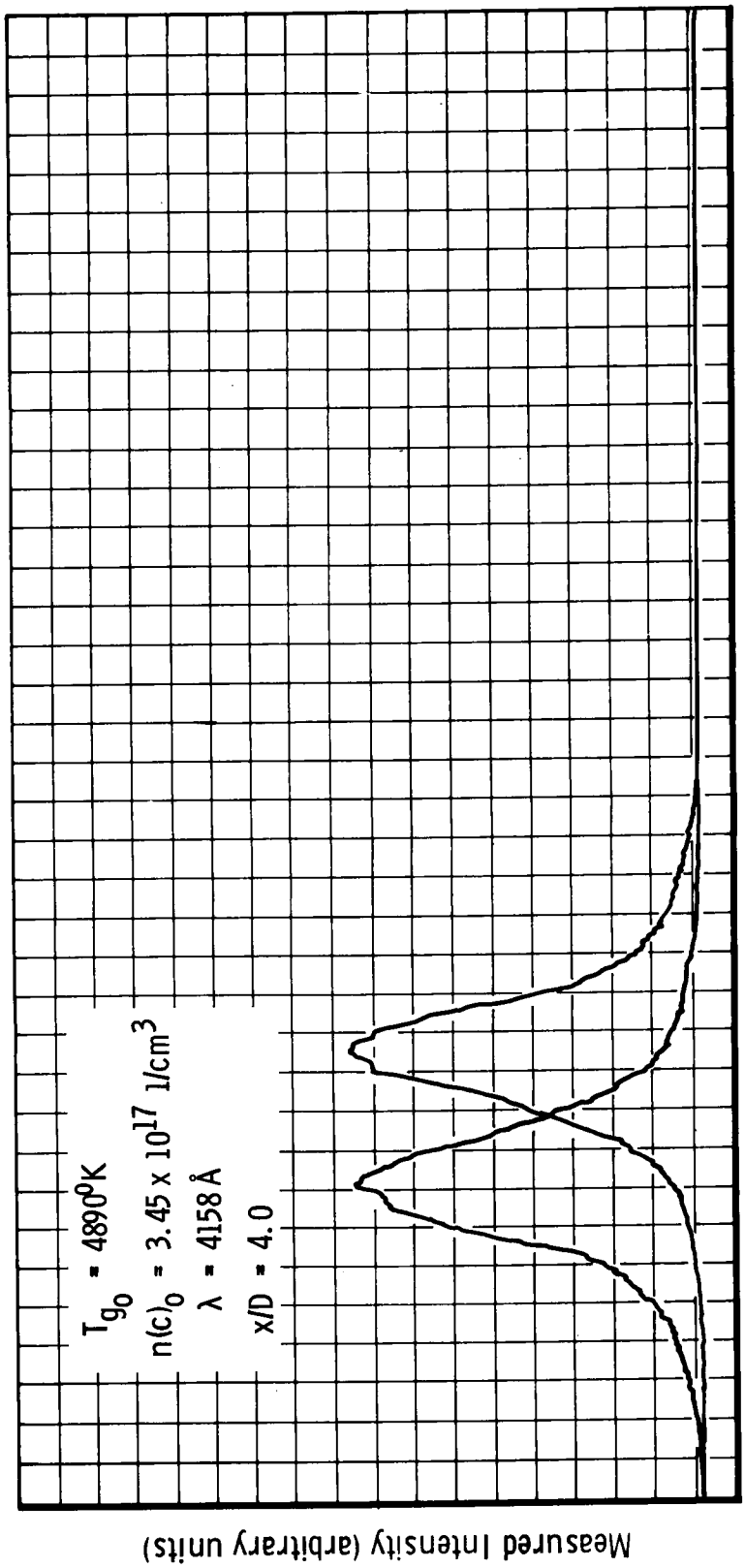

Figure 13. Raw data (intensity) scans for a wavelength of 4158 Å at a position (x/D) of 4.0.

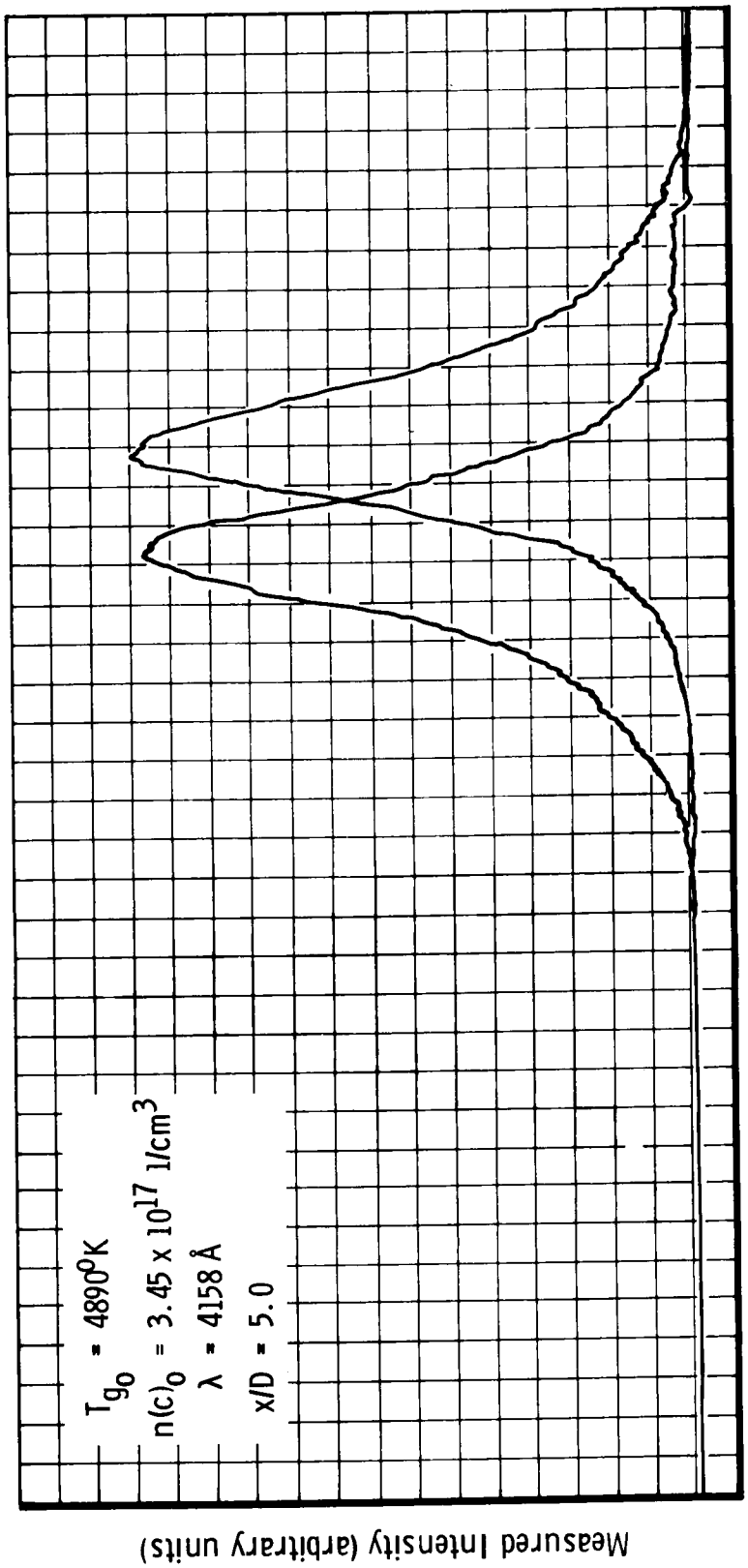

Figure 14. Raw data (intensity) scans for a wavelength of 4158 Å at a position (x/D) of 5.0.

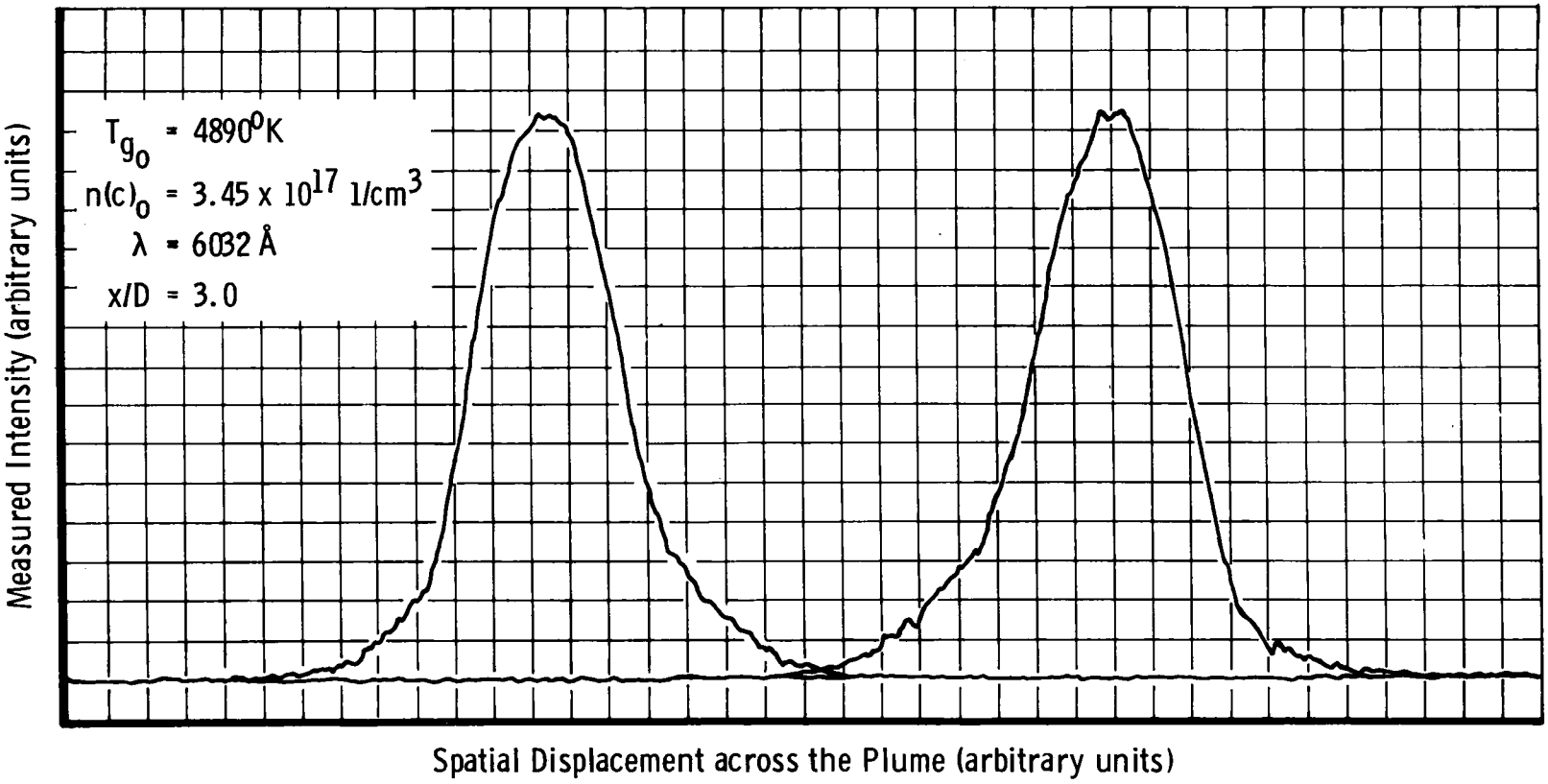

Figure 15. Raw data (intensity) scans for a wavelength of 6032 Å at a position (x/D) of 3.0.

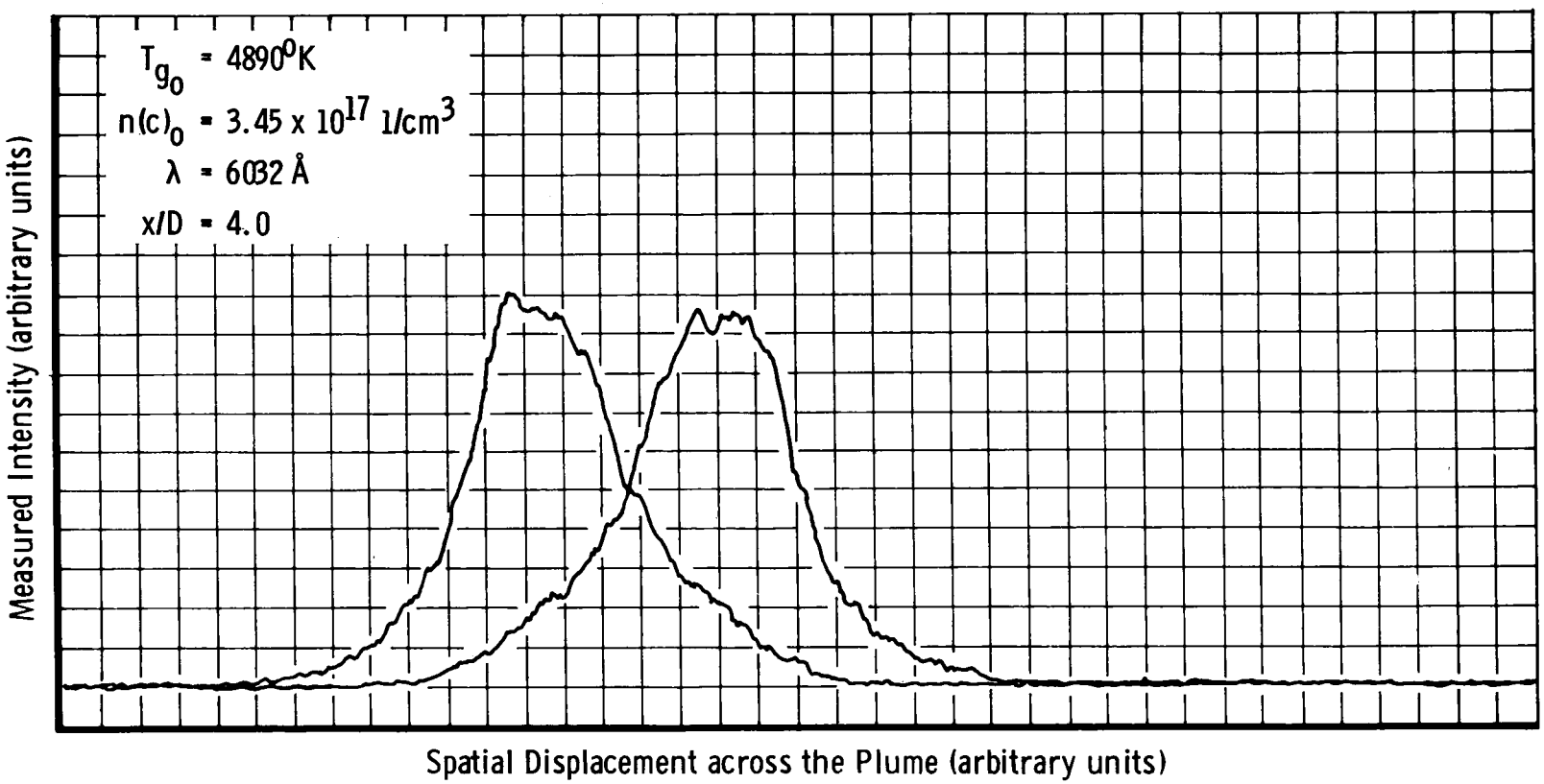

Figure 16. Raw data (intensity) scans for a wavelength of 6032 Å at a position (x/D) of 4.0.

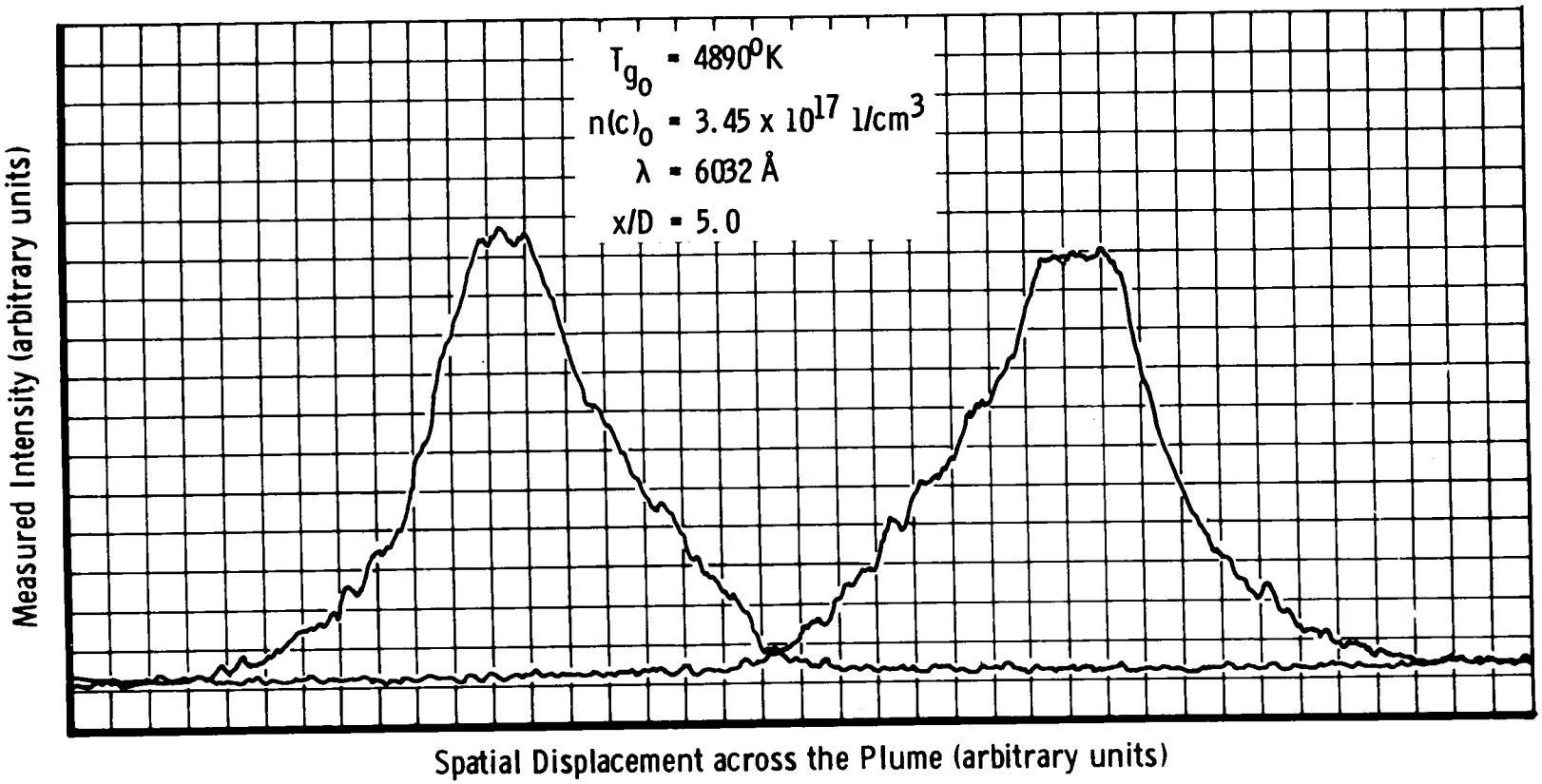

Figure 17. Raw data (intensity) scans for a wavelength of 6032 Å at a position (x/D) of 5.0.

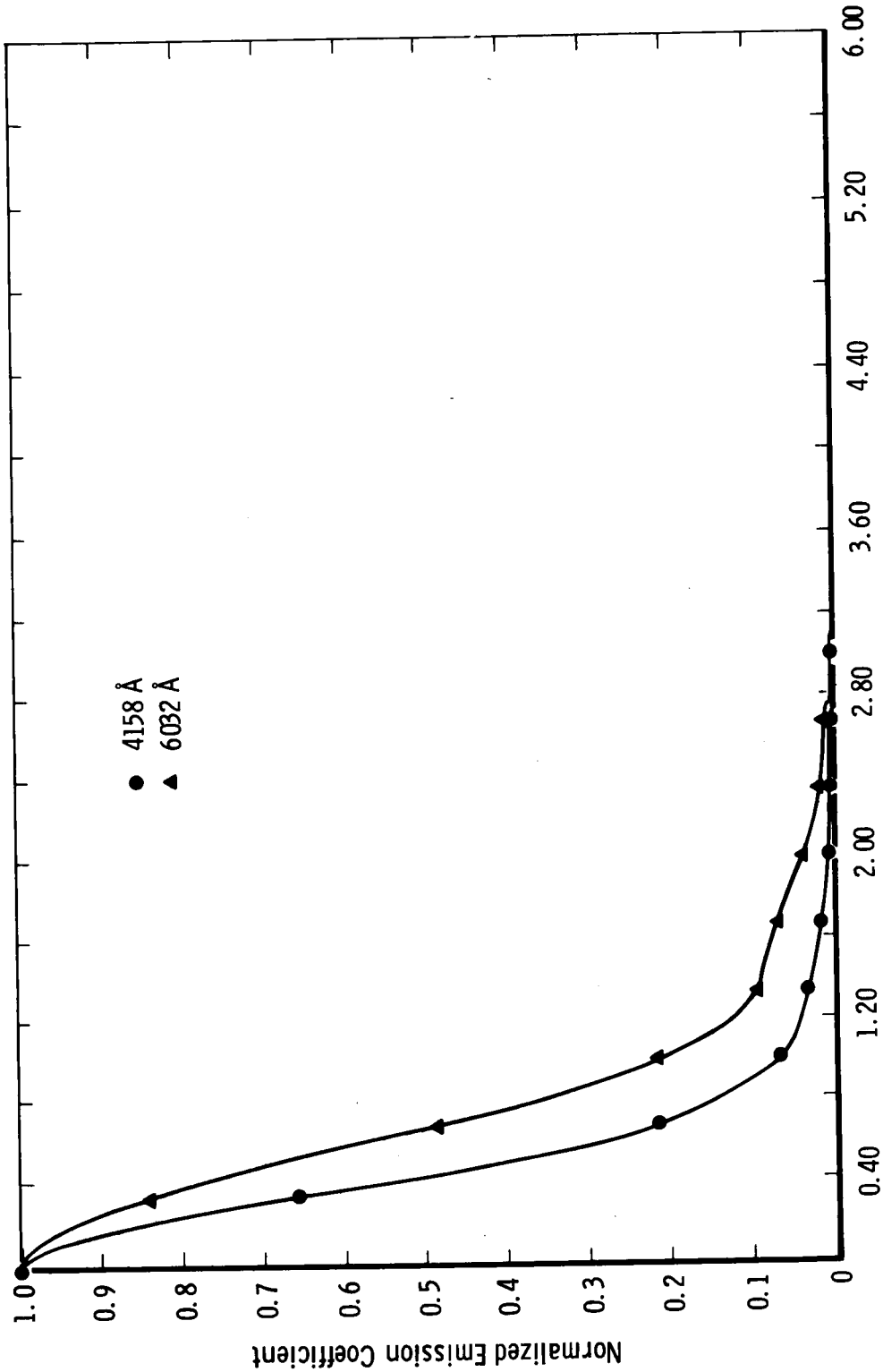

Figure 18. Normalized emission coefficient at a position (x/D) of 3.0.

is a plot of the normalized emission coefficient as determined from the above program for one of the points of measurement.

Once the emission coefficients are calculated the electron temperature is determined from the slope of a Boltzmann plot. The emission coefficient is divided by the statistical weight of the emitting state, the transition probability for the transition, and the frequency of the emitted radiation. This value is then plotted against the energy of the radiating state. These plots give straight lines of slope of $-0.4343/kT_e$, yielding immediately the electron temperature. Figure 19 is a plot of the electron temperature as determined from the emission coefficients along the centerline. The bars indicate the observed variation in the calculated electron temperature from variations in the fitted intensity data within the previously mentioned 5% variation.

The arc extends beyond the nozzle exit plane, and the conventional isentropic gas dynamic theory is not a valid approximation in this region of energy addition ($0 \leq x/D < 3.0$). In the region of the Mach disk the analysis is also invalid because of the normal shock. Beyond the region affected by the arc the electron number density will decrease due to the expansion of the gas and recombination, but at the Mach disk it will increase in this region of higher density. From the experimental data the

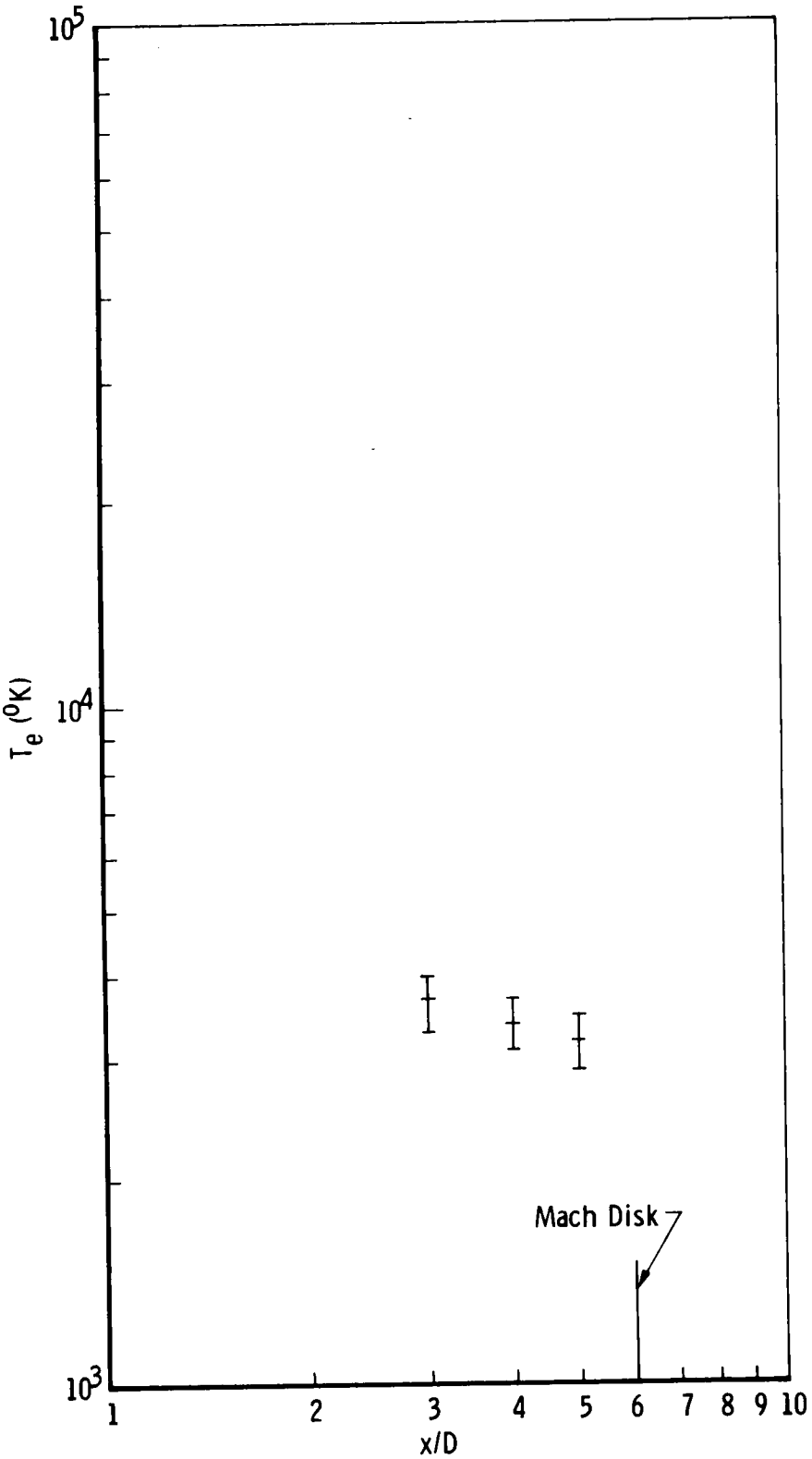

Figure 19. Electron temperature along the centerline as calculated from intensity measurement.

electron number density was observed to increase at an x/D of 6.0. Therefore, the Mach disk was judged to be located at approximately this position. For the present conditions it is estimated that the data in the region $3.0 \leq x/D < 6.0$ are amenable to the analysis used here.

With the above determined electron temperature the electron number density is obtained from Equation (17). Since the gas is assumed to be singly ionized, the ion number density and electron number density are equal. Using the above determined T_e, the n(c) can thus be determined when set in equilibrium with some excited state. These results are plotted in Figure 20 for the electron number density along the centerline data versus x/D. As with the electron temperature, only the region $3.0 \leq x/D < 6.0$ yields valid results. The bars in Figure 20 have the same meaning as in Figure 19.

In Figure 20 the three data points form a straight line on the log-log plot. If gas dynamic effects are the dominant feature of the electron number density decay, the n(c) will decay according to an inverse square law; that is, on a plot such as Figure 20, will yield a straight line of slope -2. If there are any other competing phenomena for the electron number density decay, such as the recombination process, these will be in addition to the gas dynamical effects, and the log-log plot will necessarily have slope steeper than -2. The straight line slopes obtained from

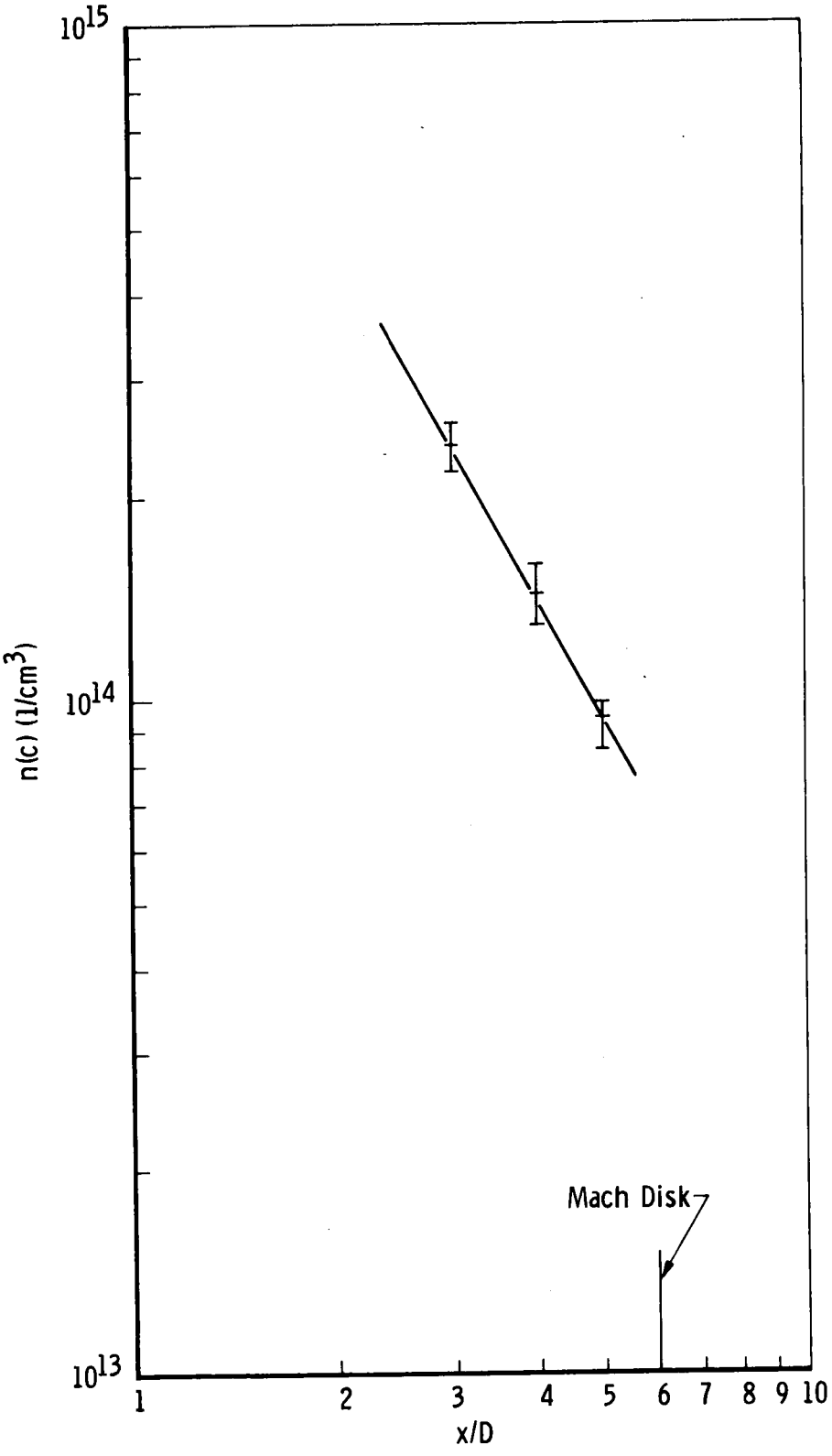

Figure 20. Electron number density along the centerline as calculated from intensity measurement.

Figure 20 have a median value of -1.8 with lower and upper bounds of -1.45 and -2.15, respectively. Thus, one is lead to the conclusion that the gas dynamical effects are the principal contributor to the electron number density decay within the resolution of the present work.

IV. THEORETICAL COMPARISONS

Due to the expansion of the gas the atom number density from the nozzle exit decreases. Also, the electron number density decreases because of both the expansion of the gas and recombination. If the recombination rate is to be observed, there should be a noticeable change in the ratio of the electron number density to the atom number density as the distance from the nozzle exit increases.

In addition to calculating Mach numbers from the characteristics solution, the mass density can be calculated by using a method of characteristics program [29]. Using the total mass density from this program the atom number density n(N) is calculated by

$$n(N) = \frac{\rho}{m_A} , \tag{48}$$

where ρ is the total mass density and m_A is the mass of an argon atom. The ratio of the electron number density to the atom number density is thus given by

$$L = \frac{n(c)}{n(N)} . \tag{49}$$

The values of L at x/D positions of 3, 4, and 5 are shown in Table IV. These values show that for the first of the three positions, L is relatively constant with a variation of only approximately 8%. The almost constant values of L imply that the degree to which recombination is affecting the electron number density must be very small compared to the gas expansion.

These results have been consistent with the theoretical predictions and analysis presented in Chapter III. However, the experimental data presented here were at a higher initial gas temperature (4890°K) while the electron number density (3.45×10^{17} $1/cm^3$) was within the range of the conditions listed in Chapter III. This higher gas temperature will affect principally the Mach number of the expansion and should not affect the conclusion of Chapter III. However, for completeness, the coupled recombination and gas dynamics program was used with the above initial conditions in order to determine if the results of theory and experiment were consistent. Figure 21 is a plot of the CRR rate and GD rate for the initial conditions of the experimental data versus time. The CRR rate does dominate in the region ($x/D < 2$) that is affected by the arc physically, and thus analysis of the

TABLE IV

Calculated Values for the Ratio (L) of Electron Number Density to Atom Number Density

x/D	n(N) ($1/cm^3$)	n(c) ($1/cm^3$)	L
3	2.42×10^{16}	2.39×10^{14}	9.88×10^{-3}
4	1.59×10^{16}	1.45×10^{14}	9.12×10^{-3}
5	1.02×10^{16}	9.47×10^{13}	9.29×10^{-3}

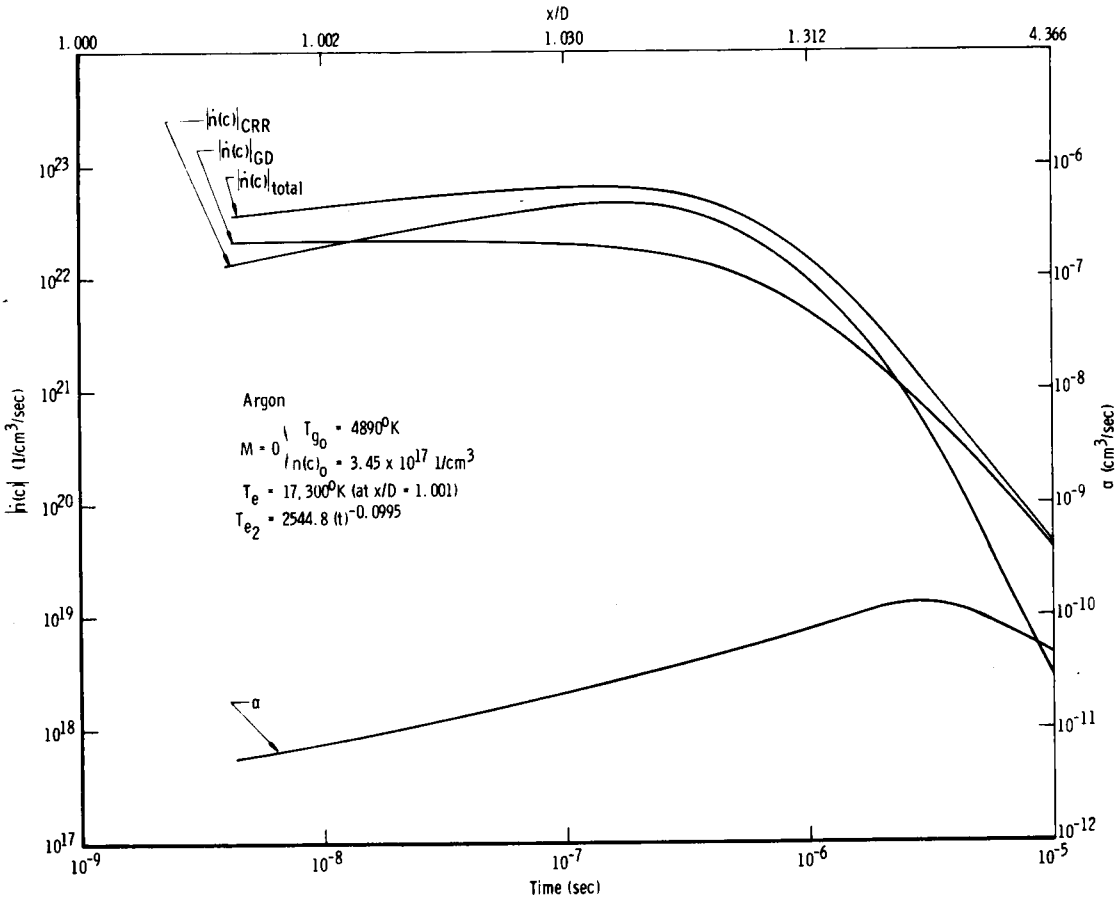

Figure 21. Collisional-radiative recombination rate and gas dynamic rate versus time; initial gas temperature of 4890°K, initial electron number density of 3.45 x 1017 1/cm^3, and electron temperature (at x/D = 1.001) of 17,300°K.

data is invalid. In the region ($3.0 \leq x/D < 6.0$) where analysis of the data is reliable, the GD rate dominates, which is consistent with the theoretical work of Chapter III and the analysis of the experimental data presented in this chapter.

CHAPTER V

SUMMARY AND CONCLUSIONS

The preceding chapters described a study of the feasibility of determinating the recombination rate coefficient of a partially ionized argon plasma through spectroscopic determination of the electron number density at successive points along the centerline of an arcjet plume. For this purpose the equations describing the recombination process were coupled with the equations describing the free isentropic expansion of an ideal gas. In this manner, calculations comparing the rate of change of the free electron number density because of recombination to the rate of change because of the gas dynamic expansion were made for a range of conditions similar to those anticipated for a typical argon arcjet plume.

In the range of stagnation conditions studied ($1300°K \leq$ gas temperature $\leq 2800°K$; $8.27 \times 10^{13} \leq$ electron number density $\leq 5.00 \times 10^{18}$ $1/cm^3$; and $8000°K \leq$ electron temperature $\leq 20{,}000°K$) the GD rate generally dominated over the CRR rate. It was further found that those conditions for which the CRR rate did dominate over the GD rate required electron number densities which are greater than those normally achieved in typical arcjet experiments. Analysis of available experimental data confirmed these

calculated results. This data analysis showed that the electron number density decay along the centerline of the plume was functionally an inverse square dependence, as is required by isentropic gas dynamical theory, and further, that the level of ionization was very nearly constant over the range of validity of the data. This latter result indicates that the recombination process did not affect the electron number density appreciably in the region studied, as it would have had to if it were an important feature of the decay.

It is thus concluded that measurements to ascertain the argon recombination rate coefficient using an arcjet will require detailed measurements to obtain excited state densities at a point on the centerline of the plume. These data and concomitant analysis can then take into account the excited state distribution function in the nonequilibrium environment of the arcjet. In this manner the quasi-steady state recombination coefficient can be determined by established methods [12]. The data would also provide the means to examine the fully transient atomic description [17] with the macroscopic gas dynamical description without recourse to the simplifying quasi-steady state assumption. In this manner the macroscopic recombination rate coefficient could be determined even in environments with rapidly varying conditions.

BIBLIOGRAPHY

BIBLIOGRAPHY

1. McDaniel, E. W. Collision Phenomena in Ionized Gases. New York: John Wiley and Sons, Inc., 1964.

2. Bates, D. R., A. E. Kingston, and R. W. P. McWhirter. "Recombination Between Electrons and Atomic Ions," Proceedings of the Physical Society of London, 267(Series A):297-312, May, 1962.

3. Biondi, M. A., and S. C. Brown. "Measurements of Ambipolar Diffusion in Helium," Physical Review, 75:1700-1705, June, 1949.

4. Biondi, M. A., and S. C. Brown. "Measurements of Electron-Ion Recombination," Physical Review, 76:1697-1700, December, 1949.

5. Oskam, H. J. "Microwave Investigation of Disintegrating Gaseous Discharge Plasmas," Philips Research Report, 13:335-400, August, 1958.

6. Redfield, A., and R. B. Holt. "Electron Removal in Argon Afterglows," Physical Review, 82:874-876, June, 1951.

7. Oskem, H. J., and V. R. Mittelstadt. "Recombination Coefficient of Molecular Rare-Gas Ions," Physical Review, 132:1445-1454, November, 1963.

8. Chen, C. J. "Collisional-Radiative Electron-Ion Recombination Rate in Rare-Gas Plasmas," Journal of Chemical Physics, 50:1560-1566, February, 1969.

9. Chen, C. J. "Partition of Recombination Energy in the Decaying Rare-Gas Plasmas," Physical Review, 163:1-7, November, 1967.

10. Gusinow, M. A., J. B. Gerado, and J. T. Verdeyen. "Investigation of Electron Recombination in Helium and Argon Afterglow Plasmas by Means of Laser Interferometric Measurements," Physical Review, 149:91-96, September, 1966.

11. Gerardo, J. B., and J. T. Verdeyen. "Correlated Interferometric Measurements of Plasma Electron Densities at Optical and Microwave Frequencies," Applied Physics Letters, 6:105-107, May, 1965.

12. Shirai, H., and K. Tabei. "Measurements of the Electronic Recombination Coefficient in a Helium Plasma Jet," Physical Review A, 7:1402-1407, April, 1973.

13. McGregor, W. K. Private communication. Arnold Engineering Development Center, Arnold Air Force Station, Tennessee, January, 1972.

14. Byron, S., R. C. Stabler, and P. I. Bortz. "Electron-Ion Recombination by Collisional and Radiative Processes," Physical Review Letters, 8:376-379, May, 1962.

15. Wanless, D. "Electron-Ion Recombination in Argon," Journal of Physics B: Atomic and Molecular Physics, 4:522-527, April, 1971.

16. D'Angelo, N. "Recombination of Ions and Electrons," Physical Review, 121:505-507, January, 1961.

17. Limbaugh, C. C. "The Transient Behavior of Collisional-Radiative Recombination in Atomic Helium Plasmas." Ph.D. dissertation, The University of Tennessee, Knoxville, 1971.

18. Bryson, R. J., and J. P. Fröhlich. "Study of the Energy Addition Process in a D-C Arc Jet," Arnold Engineering Development Center TR-65-268, Arnold Air Force Station, Tennessee, April, 1966.

19. Shapiro, A. H. The Dynamics and Thermodynamics of Compressible Fluid Flow. Vol. I. New York: The Ronald Press Company, 1954.

20. White, A. B. Part I. "Experimental Investigation of an Arc-Heated Supersonic Free Jet." Part II. "Analysis of One-Dimensional Isentropic Flow for Partially Ionized Argon." Ph.D. dissertation, California Institute of Technology, Pasadena, 1967.

21. Ashkenas, H., and F. S. Sherman. "The Structure and Utilization of Supersonic Free Jets in Low Density Wind Tunnels," Rarefied Gas Dynamics, J. H. de Leeuw, editor. Supplement 3, Vol. II. New York: Academic Press, Inc., 1966. Pp. 84-105.

22. Limbaugh, C. C. Private communication. Arnold Engineering Development Center, Arnold Air Force Station, Tennessee, January, 1973-November, 1974.

23. McGregor, W. K., and L. E. Brewer. "Equivalence of Electron and Excitation Temperatures in an Argon Plasma," Research Notes, The Physics of Fluids, 9:826-827, April, 1966.

24. Bryson, R. J. Private communication. Arnold Engineering Development Center, Arnold Air Force Station, Tennessee, August, 1973.

25. Few, J. D. Private communication. Arnold Engineering Development Center, Arnold Air Force Station, Tennessee, August, 1973.

26. Brewer, L. E. "Plasma Radiation Resulting from an Overpopulation of Atoms in the Metastable State." Unpublished Master's thesis, The University of Tennessee, Knoxville, 1965.

27. McGregor, W. K. "Examination of the Conservation Laws in a Particular Class of Collisions of the Second Kind." Ph.D. dissertation, The University of Tennessee, Knoxville, 1969.

28. Griem, H. R. Plasma Spectroscopy. New York: McGraw-Hill Book Company, Inc., 1969.

29. Fox, J. H. "An Axially Symmetric, Inviscid, Real Gas, Non-isoenergetic Flow Solution by the Method of Characteristics." Unpublished Master's thesis, The University of Tennessee, Knoxville, 1968.

VITA

Lynn Hugh Malone was born on March 19, 1949, to Mr. and Mrs. John H. Malone. He was reared in Madison, Tennessee, and received his elementary and secondary education in the Davidson County-Nashville School System.

He enrolled in Middle Tennessee State University in September, 1967, and received the degree of Bachelor of Science in Physics with minors in mathematics and chemistry in May, 1971. In September, 1971, he accepted a research assistantship at The University of Tennessee Space Institute, and in March, 1975, he received the degree of Master of Science with a major in Physics.